JOURNAL OF VIROLOGY, Sept. 2007, p. 8953–8966 Vol. 81, No. 17
0022-538X/07/$08.00+0 doi:10.1128/JVI.00649-07

Hepatitis C Virus Nonstructural Protein 5A Modulates the Toll-Like Receptor-MyD88-Dependent Signaling Pathway in Macrophage Cell Lines▽

Takayuki Abe,[1] Yuuki Kaname,[1] Itsuki Hamamoto,[1]† Yoshimi Tsuda,[1]‡ Xiaoyu Wen,[1] Shuhei Taguwa,[1] Kohji Moriishi,[1] Osamu Takeuchi,[2] Taro Kawai,[2] Tatsuya Kanto,[3,4] Norio Hayashi,[3] Shizuo Akira,[2] and Yoshiharu Matsuura[1]*

Department of Molecular Virology,[1] and Department of Host Defense,[2] Research Institute for Microbial Diseases, and Department of Gastroenterology and Hepatology,[3] and Department of Dendritic Cell Biology and Clinical Applications,[4] Graduate School of Medicine, Osaka University, Osaka, Japan

Received 27 March 2007/Accepted 6 June 2007

Hepatitis C virus (HCV) infection induces a wide range of chronic liver injuries; however, the mechanism through which HCV evades the immune surveillance system remains obscure. Blood dendritic cells (DCs) play a pivotal role in the recognition of viral infection and the induction of innate and adaptive immune responses. Several reports suggest that HCV infection induces the dysfunction of DCs in patients with chronic hepatitis C. Toll-like receptor (TLR) has been shown to play various roles in many viral infections; however, the involvement of HCV proteins in the TLR signaling pathway has not yet been precisely elucidated. In this study, we established mouse macrophage cell lines stably expressing HCV proteins and determined the effect of HCV proteins on the TLR signaling pathways. Immune cells expressing NS3, NS3/4A, NS4B, or NS5A were found to inhibit the activation of the TLR2, TLR4, TLR7, and TLR9 signaling pathways. Various genotypes of NS5A bound to MyD88, a major adaptor molecule in TLR, inhibited the recruitment of interleukin-1 receptor-associated kinase 1 to MyD88, and impaired cytokine production in response to TLR ligands. Amino acid residues 240 to 280, previously identified as the interferon sensitivity-determining region (ISDR) in NS5A, interacted with the death domain of MyD88, and the expression of a mutant NS5A lacking the ISDR partially restored cytokine production. These results suggest that the expression of HCV proteins modulates the TLR signaling pathway in immune cells.

Hepatitis C virus (HCV) belongs to the family *Flaviviridae* and possesses a positive, single-stranded RNA genome that encodes a single polyprotein composed of approximately 3,000 amino acids. HCV polyprotein is processed by host and viral proteases, resulting in 10 viral proteins. Viral structural proteins, including the capsid protein and two envelope proteins, are located in the N-terminal one-third of the polyprotein, followed by nonstructural proteins. HCV infects 170 million people worldwide and frequently leads to cirrhosis and hepatocellular carcinoma (36). In over one-half of patients, acute infection evolves into a persistent carrier state, presumably due to the ability of HCV to incapacitate the activation of the host immune mechanisms. Dendritic cells (DCs) are one type of potent antigen-presenting cell in vivo and play a crucial role in the enhancement and regulation of cell-mediated immune reactions. Since DCs express various costimulatory and/or adhesion molecules, they can activate even naïve T cells in a primary response. The role of the response of HCV antigen-specific T cells in viral clearance or persistence has been investigated extensively in both humans and chimpanzees (6, 27, 48, 51). These studies suggest that acute HCV infections followed by viral clearance are associated with a high frequency of HCV-specific $CD4^+$ and $CD8^+$ T-cell responses that can persist (27, 51), while chronic HCV infections are characterized by weak and restricted $CD4^+$ and $CD8^+$ T-cell responses that are not sustained (51).

Toll-like receptors (TLRs) are membrane-bound receptors that can be activated by the binding of molecular structures conserved among families of microbes. More than 10 different TLRs have been identified to date (2). They are highly conserved among mammals and are expressed in a variety of cell types. TLR binding and stimulation by pathogen-associated molecules is followed by a cascade of intracellular events that culminate in the expression of multiple genes (2). TLR signaling is mediated primarily by the adaptor protein myeloid differentiation factor 88 (MyD88), which triggers the activation of transcription factors, such as NF-κB, that are essential for the expression of proinflammatory cytokine genes (2). This pathway also leads to the potent production of type I interferon (IFN) through the activation of IFN regulatory factor 7 (IRF7) upon stimulation of TLR7 or TLR9 (22). In contrast, Toll/interleukin-1 (IL-1) receptor homology domain-containing adaptor-inducing IFN-β (TRIF/TICAM-1) mediates the production of type I IFNs primarily through the activation of IRF3 in response to TLR3 or TLR4 stimulation (2). Type I IFN induces the maturation of DCs by increasing both the expression of costimulatory molecules such as CD80, CD86, and CD40 and antigen presentation via major histocompatibility

* Corresponding author. Mailing address: Research Center for Emerging Infectious Diseases, Research Institute for Microbial Diseases, Osaka University, 3-1 Yamada-oka, Suita, Osaka 565-0871, Japan. Phone: 81-6-6879-8340. Fax: 81-6-6879-8269. E-mail: matsuura@biken.osaka-u.ac.jp.

† Present address: Infectious Disease Surveillance Center, National Institute of Infectious Diseases, Tokyo, Japan.

‡ Present address: Department of Disease Control, Graduate School of Veterinary Medicine, Hokkaido University, Sapporo 060-0818, Japan.

▽ Published ahead of print on 13 June 2007.

complex class I in addition to classical endogenous antigen presentation; it also facilitates the cross-presentation of viral antigens. A cumulative report has shown that DC activation via TLR signaling is a prerequisite for the subsequent induction of vigorous T-cell responses (42). Some viral proteins have been shown to inhibit the TLR-dependent signaling pathway through interactions with the downstream adaptor molecules, suggesting that the alteration of TLR-mediated signals is one of the mechanisms of virus-induced immune modulation (49). Dysfunction of DCs in patients with chronic HCV infection due to immaturation caused by the direct infection of DCs by HCV or by interactions with HCV proteins has been reported previously (4, 21). On the other hand, there have also been contrasting reports suggesting a lack of impairment of DC function in both chimpanzees and humans chronically infected with HCV (26, 32). Thus, at present, alterations in the TLR signaling pathway in the immune cells of patients with chronic hepatitis C virus infection are not well understood.

In the present study, we examined the effect of HCV proteins on TLR function in murine macrophage cell lines stably expressing HCV proteins. The expression of NS3, NS3/4A, NS4B, or NS5A was found to impair the activation of the TLR signaling pathways, and NS5A interacted with MyD88 through the IFN sensitivity-determining region (ISDR) and impaired cytokine production. To the best of our knowledge, this is the first demonstration of NS5A as an immunomodulator of TLR signaling pathways through the direct interaction with an adaptor molecule in immune cells.

MATERIALS AND METHODS

Cell culture. Human embryonic kidney 293T cells and mouse macrophage RAW264.7 cells were maintained in Dulbecco's modified Eagle's medium (Sigma, St. Louis, MO) containing 10% fetal calf serum. All cells were cultured at 37°C in a humidified atmosphere with 5% CO_2.

Plasmids and viruses. DNA fragments encoding each of the HCV structural and nonstructural proteins were generated from a full-length cDNA clone of genotype 1b strain J1 (1) by PCR using *Pfu* Turbo DNA polymerase (Stratagene, La Jolla, CA). The fragments were cloned into pCAGGs-puro/N-Flag, in which the sequence encoding a Flag tag is inserted at the 5′ terminus of the cloning site of pCAGGs-puro (37). A protease-deficient NS3/4A mutant with Ser^{139} replaced with Ala (S139A) was generated by the method of splicing by overlap extension and cloned into pCAGGs-puro. NS5A genes were amplified by PCR from HCV clones of strains of J1 (genotype 1b), H77c (genotype 1a, kindly provided by J. Bukh), and JFH1 (genotype 2a, kindly provided by T. Wakita) and cloned into pcDNA3.1Flag/HA (38). The NS5A deletion mutants were prepared as described previously (16). DNA fragments encoding a human MyD88, human Toll–IL-1 receptor domain-containing adapter protein (TIRAP), and human TRIF-related adapter molecule (TRAM) were amplified by reverse transcription-PCR from total RNA of THP-1 cells and cloned into pcDNA3.1-C-Myc-His (Invitrogen, Carlsbad, CA) and pcDNA3.1Flag/HA. Murine IPS-1 (mIPS-1) was amplified from total RNA of RAW264.7 cells by reverse transcription-PCR and cloned into pcDNA3.1Flag/HA. Human MyD88 deletion mutants and a mIPS-1 mutant with Cys^{508} replaced by Ala (C508A) were generated by the method of splicing by overlap extension and cloned into pcDNA3.1Flag/HA. pCMVIRAK1-myc and pCMVIRAK4-myc, encoding IL-1 receptor-associated kinase 1 (IRAK-1) and IRAK-4, respectively, were prepared as described previously (53). pEFBossTICAM-1-HA was kindly provided by T. Seya (44). All PCR products were confirmed by sequencing by using an ABI PRSM 310 genetic analyzer (Applied Biosystems, Tokyo, Japan). Vesicular stomatitis virus (VSV) (Indiana strain, NCP12.1) (19) was kindly provided by M. A. Whitt.

Establishment of stable cell lines expressing HCV proteins. pCAGGs-puro/N-Flag plasmids encoding HCV proteins were transfected into RAW264.7 cells by liposome-mediated transfection using Lipofectamine 2000 (Invitrogen) and selected with 10 μg/ml of puromycin (InvivoGen, San Diego, CA). After about 2 to 3 weeks of selection, several clones were isolated, and cell lysates of each clone were immunoblotted with each of specific mouse anti-HCV antibody (1) or anti-Flag M2 mouse monoclonal antibody (Sigma). Macrophage cell lines stably expressing HCV proteins and a control cell line obtained by transfection with an empty pCAGGs-puro vector were maintained in the presence of puromycin (10 μg/ml) throughout the experiments.

Immunoprecipitation and immunoblotting. Cells were seeded onto a six-well tissue culture plate 24 h before transfection. The plasmids were transfected by the lipofection method, and the cells were harvested at 48 h posttransfection, washed three times with 1 ml of ice-cold phosphate-buffered saline (PBS), and suspended in 0.4 ml lysis buffer containing 20 mM Tris-HCl (pH 7.4), 135 mM NaCl, 1% Triton X-100, 10% glycerol, and protease inhibitor cocktail tablets (Roche Molecular Biochemicals, Mannheim, Germany). Cell lysates were incubated for 30 min at 4°C and centrifuged at 14,000 × *g* for 15 min at 4°C. The supernatant was immunoprecipitated with 1 μg of mouse monoclonal anti-Flag M2, anti-hemagglutinin (HA) 16B12 (HA.11; BabCO, Richmond, CA), or anti-hexahistidine (Santa Cruz Biotechnology, Santa Cruz, CA) antibody and 10 μl of protein G-Sepharose 4B Fast Flow beads (Amersham Pharmacia Biotech, Franklin Lakes, NJ) at 4°C for 90 min. The immunocomplex was precipitated with the beads by centrifugation at 5,000 × *g* for 1 min and then washed five times with 0.4 ml of 20 mM Tris-HCl (pH 7.4) containing 135 mM NaCl and 0.05% Tween 20 (TBST buffer) by centrifugation. The proteins binding to the beads were boiled in 20 μl of sample buffer and then subjected to sodium dodecyl sulfate–12.5% polyacrylamide gel electrophoresis and transferred onto polyvinylidene difluoride membranes (Millipore, Tokyo, Japan). The membranes were blocked with TBST containing 5% skim milk at room temperature for 1 h; incubated with mouse monoclonal anti-Flag M2, anti-HA 16B12, or anti-hexahistidine monoclonal antibody at room temperature for 1 h; and then incubated with horseradish peroxidase-conjugated anti-mouse immunoglobulin G (IgG) antibody at room temperature for 1 h. The cell lines (2 × 10^6 cells/well) were stimulated with various doses of lipopolysaccharide (LPS) derived from *Salmonella enterica* serovar Minnesota (Re-595) (Sigma), peptidoglycans (PGN) derived from *Staphylococcus aureus* (Sigma), R-837 (InvivoGen), or phosphorothioate-stabilized mouse CpG (mCpG) oligodeoxynucleotides (ODN1668) (TCC-ATG-ACG-TTC-CTG-ATG-CT) (Invitrogen) for the times indicated, and the phosphorylation status of extracellular signal-regulated kinase (ERK) was determined by immunoblotting using antibodies specific to ERK1/2 or phosphorylated ERK1/2 (T202/Y204) (Cell Signaling Technology, Inc., Beverly, MA). Cells (1 × 10^6 cells/well) were treated with various doses of mouse IFN-α (PBL Biomedical Laboratories, New Brunswick, NJ) or VSV for 24 h, and the phosphorylation status of double-stranded RNA-dependent protein kinase (PKR) and signal transducer and activator of transcription 1 (STAT1) was determined by immunoblotting using antibodies specific to STAT1 (Cell Signaling), phosphorylated STAT1 (Cell Signaling), or phosphorylated PKR (BioSource International, Inc., Camarillo, CA). The immune complexes were visualized with Super Signal West Femto substrate (Pierce, Rockford, IL) and detected by using an LAS-3000 image analyzer system (Fujifilm, Tokyo, Japan).

Cytokine production and enzyme-linked immunosorbent assay (ELISA). To evaluate cytokine production in macrophage cell lines expressing HCV proteins, cells were seeded onto 96-well plates at a concentration of 1 × 10^5 cells/well and stimulated with various doses of LPS, PGN, R-837, or mCpG. After 24 h of incubation, culture supernatants were collected, and IL-6 production was determined by using an OptEIA mouse IL-6 set purchased from BD Pharmingen (San Diego, CA).

Real-time PCR. The cell lines (3 × 10^6 cells/well) were stimulated with R-837, LPS, PGN, mCpG, VSV, and polyinosine-poly(C) [poly(I:C)] (Invivogen) for the times indicated, and the expression of mRNA of cytokines, chemokines, and TLR genes was determined by real-time PCR. Total RNA was prepared from the macrophage cell lines using an RNeasy Mini kit (QIAGEN). First-strand cDNA was synthesized using a ReverTra Ace (TOYOBO, Japan) and oligo(dT)$_{20}$ primer. Each cDNA was estimated by Platinum SYBR Green qPCR SuperMix UDG (Invitrogen) according to the manufacturer's protocol. Fluorescent signals were analyzed by using an ABI PRISM 7000 apparatus (Applied Biosystems). Mouse Ccl2, IFN-β, IFN-α1, IFN-α4, and IL-1-α genes were amplified with primer pairs 5′-GCATCCACGTGTTGGCTCA-3′ and 5′-CTCCAGCCTACTCATTGGGATCA-3′, 5′-ACACCAGCCTGGCTTCCATC-3′ and 5′-TTGGAGCTGGAGCTGCTTATAGTTG-3′, 5′-AGCCTTGACACTCCTGGTACAAATG-3′ and 5′-TGGGTCAGCTCACTCAGGACA-3′, 5′-GCTCAAGCCATCCTTGTGCTAA-3′ and 5′-CATTGAGCTGATGGAGGTC-3′, and 5′-TTGGTTAAATGACCTGCAACAGGA-3′ and 5′-AGGTCGGTCTCACTACCTGTGATG-3′, respectively. The mouse TLR2, TLR3, TLR4, TLR7, TLR9, and GAPDH (glyceraldehyde-3-phosphate dehydrogenase) genes were amplified using primer pairs 5′-AGCTCTTTGGCTCTTCTG-3′ and 5′-AGAACTGGGGGATATGC-3′, 5′-AAATCCTTGCGTTGCGAAGTG-3′ and 5′-TCAGTTGGGCGTTGTTCAAGAG-3′, 5′-GCCTCGAATCCTGAGCAAACA-3′ and 5′-CTTCTGCCCGGTAAGGTCCA-3′, 5′-TCTGCAGGAGCTCTGTCCTTGA-3′ and 5′-CAAGGCATGTCCTAGGTGGTGA-3′, 5′-ACCAATGGCACCCTGCCTAA-3′ and 5′-

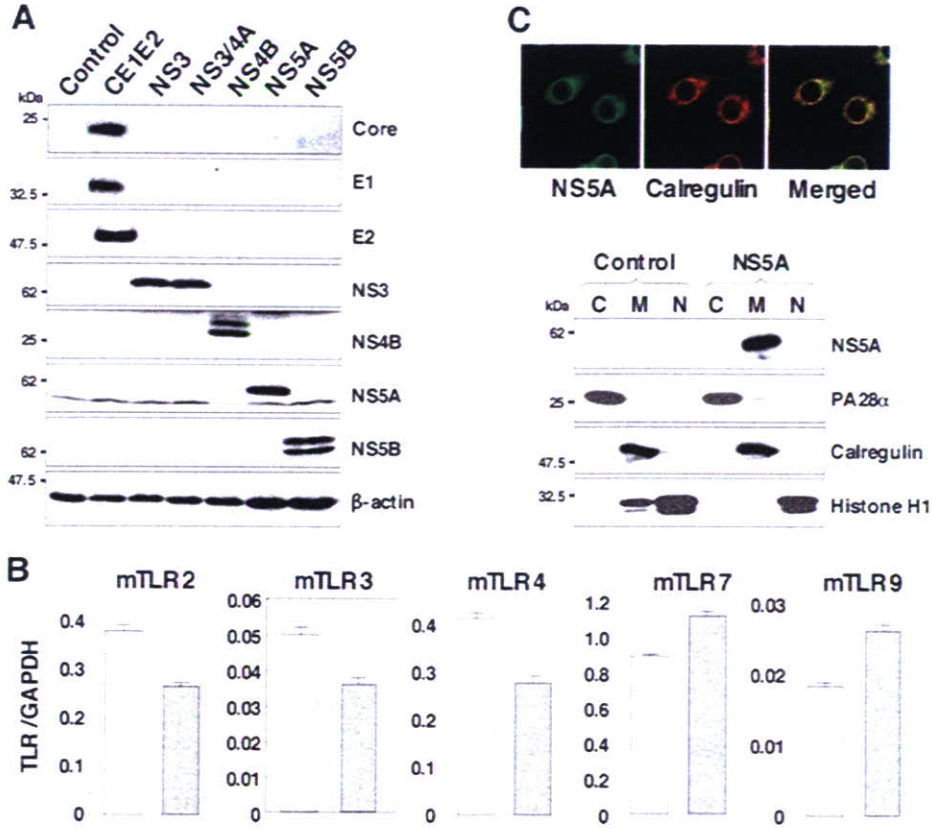

FIG. 1. Establishment of stable macrophage cell lines expressing HCV proteins. (A) Cell lysates were prepared from macrophage cell lines expressing each of the HCV proteins (4×10^6 cells) and immunoblotted with antibodies against HCV proteins or β-actin. (B) Total RNA was extracted from macrophage cell lines expressing NS5A (gray bars) or control (white bars), and the expression of mRNA of TLRs was determined by real-time PCR. (C) The subcellular localization of NS5A was examined by confocal microscopy. Cells were fixed with 4% paraformaldehyde–PBS, permeabilized with 0.5% Triton X-100, and stained with specific antibodies. Cells expressing NS5A or control cells were extracted into cytosol (C), membrane-organelle (M), and nuclear (N) fractions. Each fraction was concentrated and subjected to immunoblotting with specific antibodies. PA28α, calregulin, and histone H1 were used as markers for cytosol, membrane-organelle, and nuclear fractions, respectively.

CGTCTTGAGAATGTTGTGGCTGA-3′, and 5′-ACCACAGTCCATGCCATC AC-3′ and 5′-TCCACCACCCTGTTGCTGTA-3′, respectively. The expression of mRNAs of each of the chemokines, cytokines, and TLR was normalized with that of GAPDH mRNA.

Immunofluorescence microscopy and subcellular localization of HCV proteins in stable macrophage cell lines. Cells were seeded onto an eight-well chamber slide at 1.5×10^4 cells per well, washed twice with PBS, fixed with PBS containing 4% paraformaldehyde at 18 h of cultivation, and permeabilized with PBS containing 0.5% Triton X-100 at 15 min. The cells were then incubated at 4°C for 1 h with 1 μg of mouse anti-NS5A antibody (Austral Biologicals, San Ramon, CA) or rabbit polyclonal antibody against calregulin (Santa Cruz Biotechnology) in PBS containing 10% fetal calf serum (PBSF) and then incubated at room temperature for 1 h with 0.5 μg of Alexa Fluor 488-conjugated anti-mouse IgG (Molecular Probes) or Alexa Fluor 594-conjugated anti-rabbit IgG (Molecular Probes) after three washes with PBSF. After extensive washing with PBSF, the samples were examined with a FluoView FV1000 laser scanning confocal microscope (Olympus, Japan). To confirm the subcellular localization of the HCV proteins in the macrophage cell lines, each stable cell line was fractionated with a Subcellular Proteome Extraction kit (Calbiochem, Darmstadt, Germany). Stepwise extraction resulted in four distinct fractions, which contained primarily cytosolic, membrane-organelle, nuclear, and cytoskeleton proteins, respectively. Each fraction was concentrated by Microcon (Millipore) and subjected to immunoblotting. PA28α (Biomol International, Plymouth Meeting, PA), calregulin, and histone H1 (Santa Cruz Biotechnology) were used as cytoplasmic, membrane, and nuclear markers, respectively.

RESULTS

Establishment of macrophage cell lines stably expressing HCV proteins. To examine the effect of HCV proteins on the TLR function of immune cells, we established murine macrophage cell lines stably expressing HCV structural or nonstructural proteins. We selected mouse macrophage RAW264.7 cells due to their high level of expression of various TLRs (3) and their high sensitivity to stimulation with TLR ligands. Processed HCV structural and nonstructural proteins were detected in each of the cell lines by immunoblot analyses using specific monoclonal antibodies (Fig. 1A). To examine the effect of HCV proteins on TLR expression in macrophage cell lines, the mRNA of TLRs in cells expressing NS5A was determined by real-time PCR (Fig. 1B). Although slight reductions in TLR2, TLR3, and TLR4 or enhancement of TLR7 and TLR9 was observed, a substantial amount of mRNA of the examined TLRs was detected in the cell lines expressing NS5A and other HCV proteins (data not shown). To determine the subcellular localization of HCV proteins in macrophage cell lines, the expression of HCV proteins was examined by con-

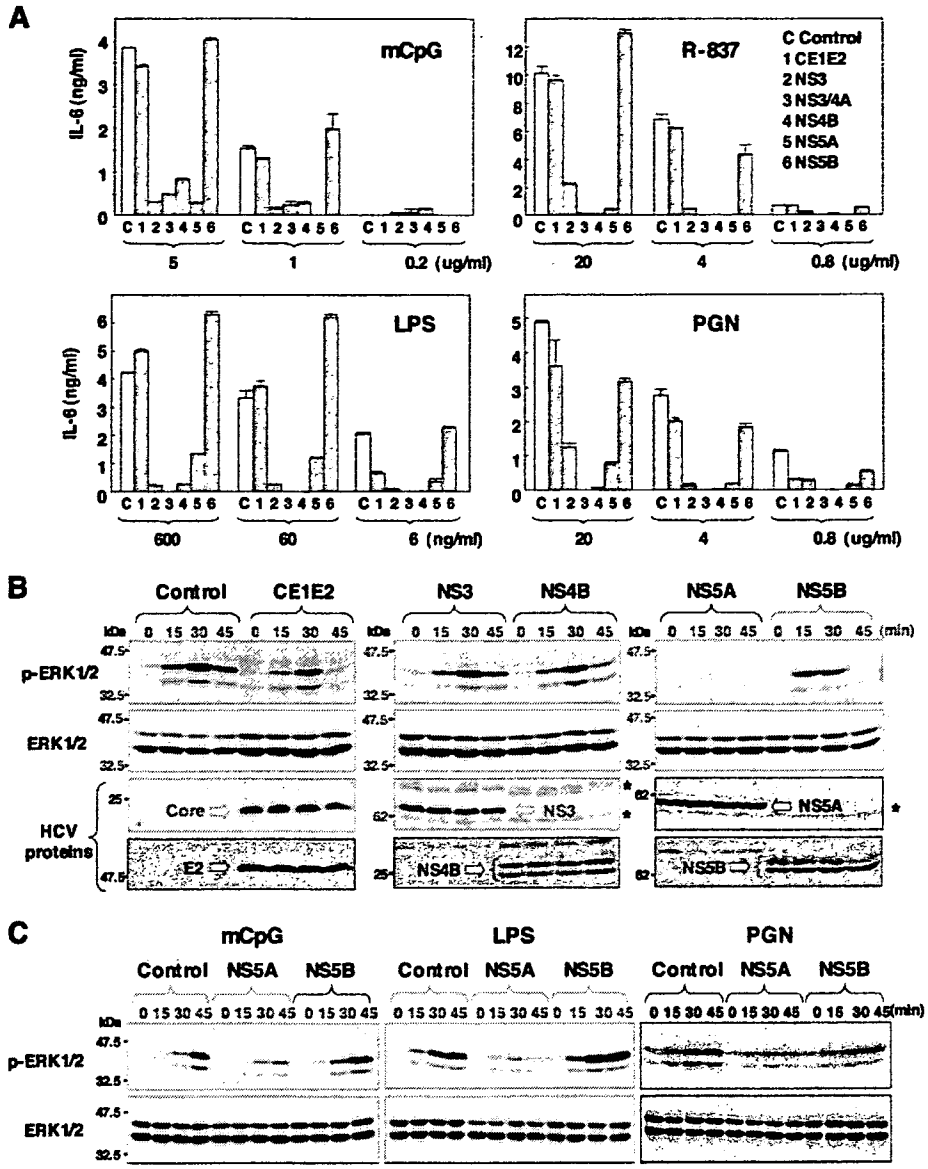

FIG. 2. Expression of HCV nonstructural proteins modulates IL-6 production and MAPK cascades through the TLR-dependent signaling pathway in macrophage cell lines. (A) Cells were seeded onto 96-well plates (1×10^5 cells/well) and stimulated with the indicated amounts of mCpG, R-837, LPS, or PGN. After 24 h of stimulation, IL-6 production in the culture supernatants was determined by sandwich ELISA. Data are shown as means ± standard deviations (SD). (B) Cells (2×10^6 cells/well) were stimulated with 10 μg/ml of R-837 for the times indicated, and ERK1/2 phosphorylation was determined by immunoblotting with antibodies to ERK and phosphorylated ERK (p-ERK). Asterisks indicate nonspecific bands. (C) Cells (2×10^6 cells/well) were stimulated with 10 μg/ml of mCpG, 25 ng/ml of LPS, or 10 μg/ml of PGN for the times indicated, and ERK1/2 phosphorylation was determined by immunoblotting.

focal microscopy and cell fractionation (Fig. 1C). HCV NS5A was colocalized with the endoplasmic reticulum marker calregulin in the macrophage cell line as reported previously for human hepatoma cell lines (47). Other HCV proteins exhibited similar localization with NS5A (data not shown). To further confirm the subcellular localization of NS5A proteins, cytoplasmic, membrane-organelle, and nuclear fractions of the cell line expressing NS5A were analyzed by Western blotting. NS5A was detected mainly in the membrane-organelle fraction.

Expression of HCV NS3, NS3/4A, NS4B, or NS5A modulates the TLR-dependent signaling pathway in macrophage cell lines. In order to determine the effect of the expression of HCV proteins on the TLR signaling pathway in macrophage cell lines, we examined the ability of HCV proteins to inhibit NF-κB activation via stimulation with various TLR ligands. The macrophage cell lines were stimulated with the TLR ligands, and the production of the proinflammatory cytokine IL-6 in the culture supernatants was determined by ELISA (Fig. 2A). The expression of HCV structural proteins or NS5B

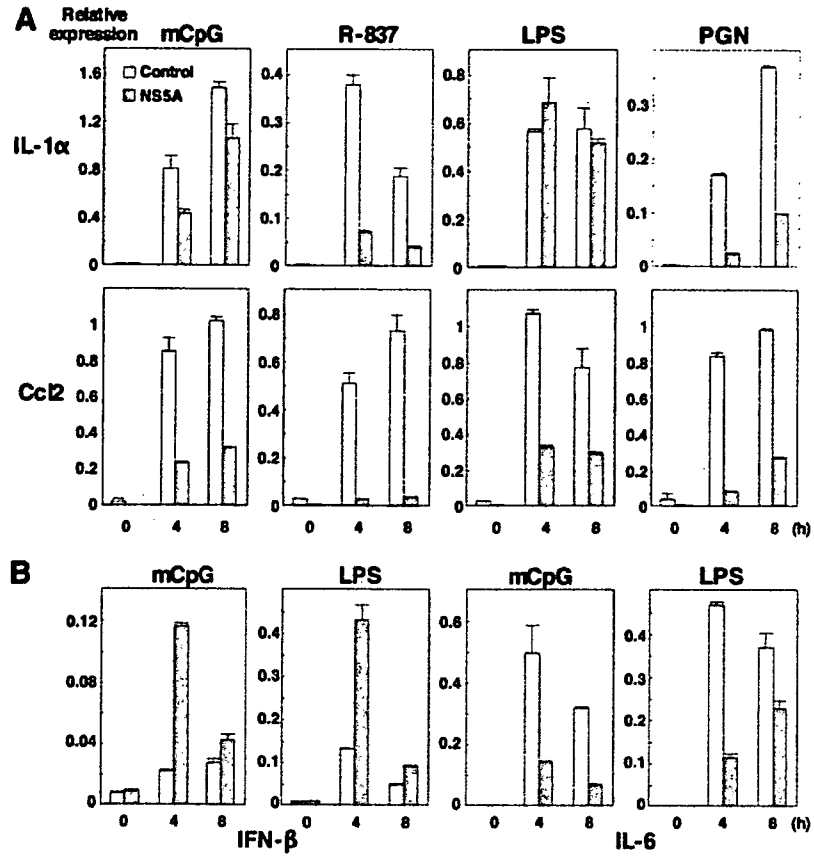

FIG. 3. Effect of NS5A expression on the production of cytokines and chemokines in response to TLR ligands in macrophage cell lines. Cells (3×10^6 cells/well) were stimulated with 10 μg/ml of mCpG, 10 μg/ml of R-837, 25 ng/ml of LPS, and 10 μg/ml of PGN for the times indicated. Total RNA was extracted from macrophage cell lines expressing NS5A (gray bars) or control (white bars), and the expression of mRNA of IL-1α and Ccl2 (A) and IFN-β and IL-6 (B) was determined by real-time PCR.

had no effect on IL-6 production after stimulation with mCpG, R-837, LPS, or PGN, which are ligands for TLR9, TLR7, TLR4, and TLR2, respectively. On the other hand, the expression of NS3, NS3/4A, NS4B, or NS5A inhibited the production of IL-6 induced by treatment with the ligands. These results indicate that the expression of NS3, NS3/4A, NS4B, and NS5A inhibits the production of IL-6 through the TLR-dependent signaling pathway in macrophage cell lines.

In addition to proinflammatory cytokine production via NF-κB activation, stimulation of TLR also activates mitogen-activated protein kinases (MAPKs). We then examined the activation of ERK, a MAPK signaling pathway, in response to the TLR ligands in the macrophage cells expressing HCV proteins (Fig. 2B). Although the expression of the HCV structural proteins NS3, NS4B, and NS5B did not alter the phosphorylation status of ERK1/2 in response to stimulation with the TLR7 ligand R-837, the expression of NS5A exhibited a clear inhibition of the phosphorylation of ERK1/2. To further examine the effect of NS5A expression on the MAPK cascade in response to the TLR ligands, the cells were treated with mCpG, LPS, and PGN. NS5A expression was found to inhibit the phosphorylation of ERK1/2 in response to stimulation with the ligands for TLR9, TLR4, and TLR2 (Fig. 2C). In contrast, the phosphorylation of c-Jun NH_2-terminal kinase in response to stimulation with R-837 was less impaired in the macrophage cell line expressing NS5A (data not shown). These results indicate that the expression of NS3, NS3/4A, NS4B, or NS5A inhibits the production of proinflammatory cytokines and that the expression of NS5A alone induces the inhibition of the MAPK cascade in response to stimulation by various TLR ligands in macrophage cells.

To further examine the effect of NS5A expression on the production of the other proinflammatory cytokines and chemokines in response to TLR ligands, the expression of mRNA of IL-1α and Ccl2 in cells expressing NS5A after stimulation with TLR ligands was determined by real-time PCR (Fig. 3A). Expression of IL-1α and Ccl2 was reduced in cells expressing NS5A by stimulation with mCpG, R-837, LPS, or PGN except for the IL-1α expression by treatment with LPS, probably due to the TRIF-dependent activation of NF-κB. To further confirm the specific inhibition of the MyD88-dependent signaling pathway by NS5A, we examined the effects of NS5A expression in macrophage cells on the MyD88-independent/TRIF-dependent production of IFN-β (Fig. 3B). Although the expression of IL-6 mRNA in cells expressing NS5A was impaired after stimulation with mCpG or LPS, the expression of IFN-β was enhanced. These results suggest that the expression of NS5A specifically inhibits the MyD88-dependent signaling pathway.

TLR-dependent and -independent immune activation of macrophage cells expressing NS3/4A or NS5A protein by RNA virus and dsRNA. TLR3 has been shown to sensitize cells in response to double-stranded RNA (dsRNA) generated by viral infection and a synthetic dsRNA analog, poly(I:C), through an adaptor molecule, TRIF/TICAM-1, but not MyD88. Furthermore, RIG-I and MDA5 have been identified as being cytoplasmic dsRNA detectors responding to poly(I:C) and viral RNAs (57, 58), sensitizing cells through an adaptor molecule, IPS-1/MAVS/VISA/CARDIF, in a TLR-independent manner (24, 35, 46, 55). Recently, HCV NS3/4A protease was shown not only to cleave HCV nonstructural proteins but also to inhibit viral RNA- and dsRNA-induced IFN production through the cleavage of the adaptor molecules TRIF (28) and IPS-1 (29, 30, 33, 35). Moreover, it has been shown that NS3/4A protease inhibits dsRNA-induced immune activation in a protease-dependent manner in human hepatoma cell lines (11).

To determine whether murine TRIF (mTRIF) is cleaved by HCV NS3/4A protease, C-terminally His-tagged mTRIF was coexpressed with N-terminally Flag-tagged NS3, NS3/4A, or NS3/4A(S139A) in 293T cells. Immunoblot analyses revealed that mTRIF was not processed by HCV NS3/4A protease, probably due to differences in the amino acid sequences at the cleavage site in mTRIF (Fig. 4A). Amino acid sequences at the cleavage site of human TRIF are Cys^{372} and Ser^{373}, and those at the cleavage sites of mTRIF are Pro^{372} and Ala^{373} (Fig. 4B). These results suggest that HCV NS3/4A protease could not inhibit immune activation through the TLR3-mTRIF-dependent signaling pathway in murine cells. We next determined the processing of IPS-1 by HCV NS3/4A protease. N-terminally Flag-tagged mIPS-1 or its C508A mutant, with Cys^{508} replaced with Ala to prevent cleavage by HCV NS3/4A protease, was coexpressed with N-terminally Flag-tagged NS3, NS3/4A, or NS3/4A(S139A) in 293T cells. Immunoblot analyses revealed that wild-type mIPS-1 was cleaved in cells coexpressing the active NS3/4A protease but not in those with NS3 (Fig. 4C). mIPS-1 processing was reduced in cells coexpressing NS3/4A(S139A) as well as in those coexpressing mIPS-1(C508A) and NS3/4A (Fig. 4C). Furthermore, we were able to detect cleavage of endogenous mIPS-1 in macrophage cell lines expressing NS3/4A but not in those expressing NS3 or NS3/4A(S139A) (Fig. 4D), indicating that mIPS-1 in murine macrophage cell lines is cleaved by HCV NS3/4A protease, as reported previously for a human hepatoma cell line.

We then examined the effect of expression of NS3/4A and NS5A on TLR-dependent and -independent immune activation induced by dsRNA. VSV and poly(I:C) were inoculated into macrophage cell lines, and the expression of mRNA of IFN-β and IL-1α was determined by real-time PCR (Fig. 4E). The macrophage cell lines expressing NS3/4A exhibited inhibition of IL-1α and IFN-β expression upon infection with VSV but not in response to poly(I:C), whereas no inhibition was observed in those expressing NS5A. These results suggest that the invasion of VSV and poly(I:C) is preferentially recognized in RAW cell lines by RIG-I–IPS-1- and TLR3-TRIF-dependent signaling pathways, respectively. Inhibition of IL-1α and IFN-β expression upon infection with VSV but not in response to poly(I:C) is probably due to the selective cleavage of IPS-1 but not TRIF by NS3/4A protease in the macrophage cell lines. In contrast, the expression of NS5A has no effect on both TLR3-TRIF and RIG-I–IPS-1-dependent signaling pathways in macrophage cells.

Although MyD88/IRF7-dependent production of IFN-α upon activation was reported in plasmacytoid DCs (pDCs) (17, 23), it is unclear whether murine macrophage cells are capable of producing IFN-α in a TLR/MyD88/IRF7-dependent manner. To examine the effect of NS5A expression on IFN-α production, the expression of IFN-α1 and IFN-α4 in the macrophage cell line upon infection with VSV was determined (Fig. 4E, bottom). In contrast to the effect on IFN-β production, the expression of NS5A in the macrophage cells reduced the production of IFN-α1 and IFN-α4 upon infection with VSV, although the inhibitory effect was weaker than that of NS3/4A. These results suggest that RAW264.7 cells are capable of producing IFN-α in a TLR/MyD88/IRF7-dependent manner upon infection with VSV as reported for pDCs, and the expression of NS5A partially counteracts this signaling pathway. However, the production of type I IFNs by the treatment with ligands for TLR7 (R-837) and TLR9 (mouse CpG) was weaker than that induced by infection with VSV in macrophage cells (data not shown). Further study is needed to clarify the precise mechanisms of the inhibition of TLR/MyD88/IRF7-dependent IFN-α production by the expression of HCV NS5A in human immune cells.

NS5A interacts with MyD88 in mammalian cells. The inhibition of the production of proinflammatory cytokines and chemokines and the MAPK cascade by NS5A expression in response to stimulation by various TLR ligands without participation of TRIF- and IPS-1-dependent signaling pathways suggests that NS5A specifically inhibits the TLR-MyD88-dependent signaling pathway in macrophage cell lines. MyD88 is a critical component of the signaling pathway and leads to the production of proinflammatory cytokines, chemokines, and MAPKs. To determine the effect of the expression of HCV proteins on the TLR signaling pathway in macrophage cell lines, the interaction of the HCV proteins with the adaptor molecules in the signaling pathway of the TLR family was examined by immunoprecipitation analysis. His-tagged MyD88 was coexpressed with Flag-tagged HCV proteins in 293T cells and immunoprecipitated with the indicated antibodies. As shown in Fig. 5A and B, MyD88 was coimmunoprecipitated with NS5A but not with structural and other nonstructural proteins in 293T cells.

To further confirm the specificity of the interaction of NS5A with MyD88, NS5A was coexpressed with other adaptor molecules in the TLR signaling pathway, TRAM, TIRAP, or TRIF, in 293T cells (Fig. 5C). NS5A interacted with MyD88 but not other adaptor molecules, suggesting that NS5A may inhibit the production of proinflammatory cytokines and chemokines and the phosphorylation of MAPKs through the counteraction of the MyD88-dependent TLR signaling pathway.

NS5A interacts with the death domain of MyD88 through the ISDR and inhibits recruitment of IRAK to MyD88. To determine the region of NS5A responsible for the interaction with MyD88, a series of deletion mutants of N-terminal Flag-tagged NS5A was constructed, and its interaction with His-tagged MyD88 was examined (Fig. 6A). The NS5A mutant covering amino acids 1 to 280 but not that covering amino

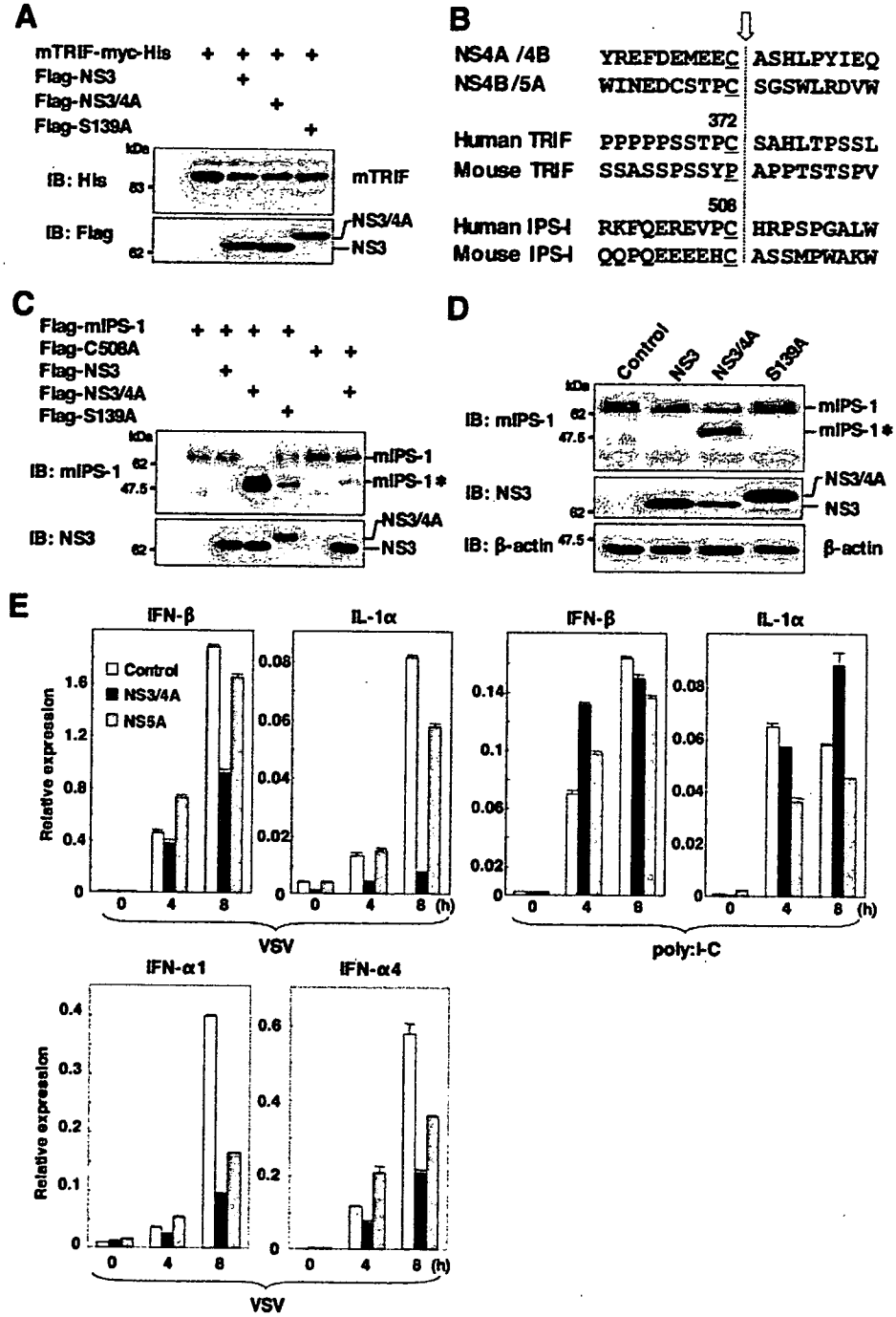

FIG. 4. TLR-dependent and -independent immune activation of macrophage cells expressing theNS3/4A or NS5A protein by RNA virus and dsRNA. (A) Myc-His-mTRIF was coexpressed with Flag-NS3, -NS3/4A, or -NS3/4A(S139A) in 293T cells and immunoblotted (IB) with antibodies against His and Flag. (B) Alignment of the flanking sequence of NS3 protease cleavage sites of NS4A/4B, NS4B/5A, TRIF, and IPS-1 of human and murine origins. The cleavage site is indicated by an arrow. (C) Flag–mIPS-1 and a mutant with Cys^{508} replaced with Ala (C508A) were coexpressed with Flag-NS3, -NS3/4A, or -NS3/4A(S139A) in 293T cells and immunoblotted with antibodies against mIPS-1 and NS3. (D) Processing of endogenous mIPS-1. Cell lysates of the macrophage cell lines expressing NS3, NS3/4A, and NS3/4A(S139A) were immunoblotted with antibodies against mIPS-1, NS3, and β-actin. The cleavage product of mIPS-1 is indicated as mIPS-I*. (E) Cells (3×10^6 cells/well) were stimulated with 2×10^5 PFU/ml of VSV or 50 μg/ml of poly(I:C) for the times indicated. Total RNA was extracted from the macrophage cell lines expressing NS3/4A (black bars), NS5A (gray bars), or control (white bars), and the expression of mRNA of IFN-β, IL-1α, IFN-α1, and IFN-α4 was determined by real-time PCR.

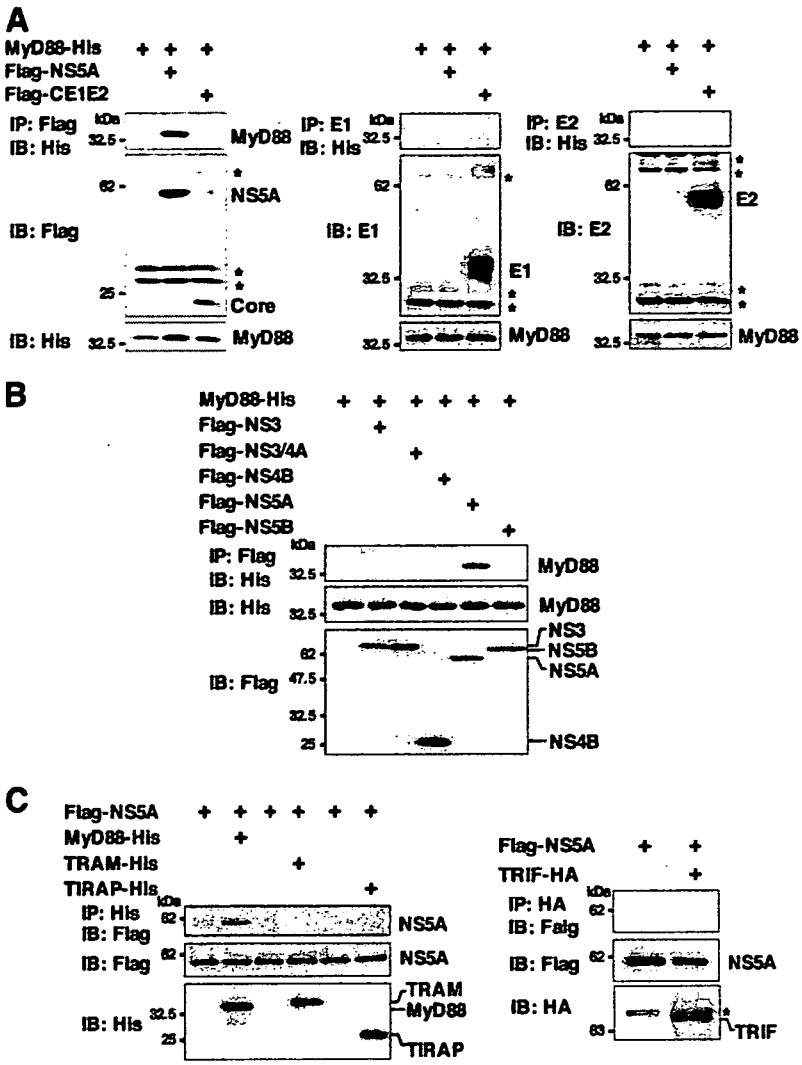

FIG. 5. NS5A interacts with MyD88. MyD88-His was coexpressed with Flag-core/E1/E2 or -NS5A (A) or Flag-NS3, -NS3/4A, -NS4B, -NS5A, or -NS5B (B) in 293T cells; immunoprecipitated (IP) with anti-Flag, E1, or E2 antibody; and immunoblotted (IB) with anti-His antibody. (C) Flag-NS5A was coexpressed with MyD88-His, TRAM-His, TIRAP-His, or TRIF-HA in 293T cells and immunoprecipitated with anti-His or -HA antibody. The immunoprecipitates were immunoblotted with anti-Flag antibody. Asterisks indicate nonspecific bands.

acids 1 to 200 exhibited binding to MyD88, suggesting that amino acid residues 200 to 280 of NS5A are required for the interaction with MyD88. Further mutational analyses of NS5A revealed that amino acid residues 240 to 280, which overlap the ISDR (amino acid residues 237 to 276), which was previously suggested to be involved in IFN resistance (10, 41), are required for the interaction with MyD88 (Fig. 6A). To determine the region of MyD88 responsible for the interaction with NS5A, His-tagged MyD88 mutants were coexpressed with Flag-tagged NS5A in 293T cells and immunoprecipitated with anti-His antibody. A MyD88 deletion mutant lacking amino acids 1 to 50, but not one lacking amino acids 1 to 80, and a mutant possessing amino acids 1 to 70 exhibited binding to NS5A, suggesting that amino acid residues 50 to 70 in the death domain of MyD88 are required for the interaction with NS5A (Fig. 6B).

MyD88 associates with TLRs and acts as an adapter that recruits IRAK, which is known as a key regulator for TLR7- and TLR9-mediated IFN-α production in pDCs (53). To determine the role of NS5A binding to MyD88 in the TLR-MyD88-dependent signaling pathway, we examined the association of IRAK with MyD88 in the presence of NS5A. Flag-tagged MyD88 was coexpressed with Myc-tagged IRAK-1 or IRAK-4 and immunoprecipitated with anti-Myc antibody (Fig. 6C, left). IRAK-1, but not IRAK-4, was coimmunoprecipitated with MyD88. Although NS5A did not bind to IRAK-1, it was not possible to assess the interaction of NS5A with IRAK-4 due to the degradation of NS5A in cells coexpressing IRAK-4 for unknown reasons (Fig. 6C, middle). To examine the interplay between IRAK-1 and MyD88 in the presence of NS5A, Flag-tagged MyD88 and Myc-tagged IRAK-1 were coexpressed with Flag-tagged NS5A in 293T cells. The interaction

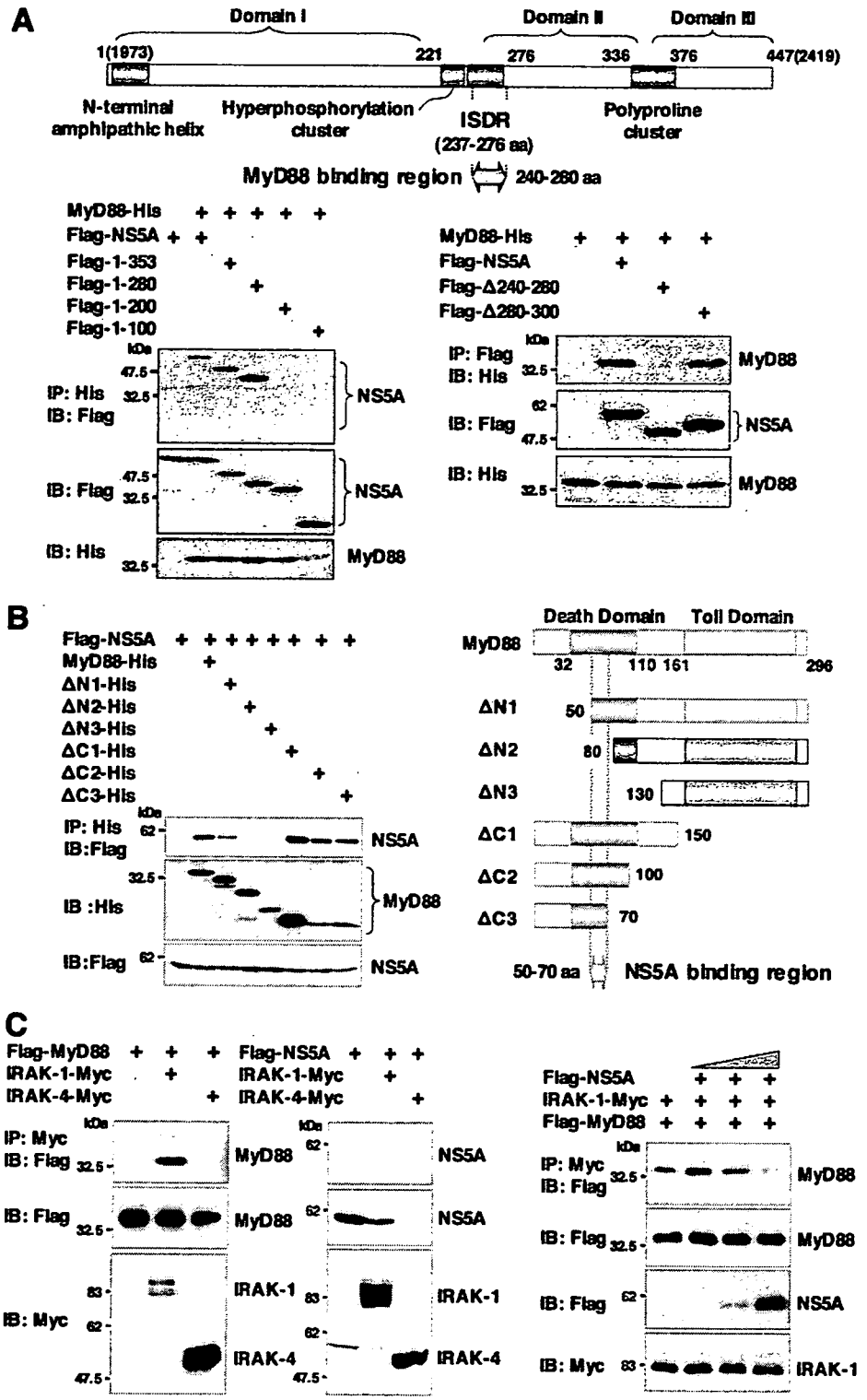

FIG. 6. NS5A interacts with the death domain of MyD88 through the ISDR and inhibits recruitment of IRAK to MyD88. (A) The structure of NS5A and the MyD88 binding region are indicated at the top. MyD88-His was coexpressed with C-terminal deletion mutants of Flag-NS5A in 293T cells, immunoprecipitated (IP) with anti-His antibody, and immunoblotted (IB) with anti-Flag antibody (left). MyD88-His was coexpressed with Flag-NS5A deletion mutants (Δ240–280 or Δ280–300) in 293T cells, immunoprecipitated with anti-Flag antibody, and then immunoblotted with anti-His antibody (right). (B) Flag-NS5A was coexpressed with N-terminal or C-terminal deletion mutants of MyD88-His (ΔN1, ΔN2, ΔN3, ΔC1, ΔC2, or ΔC3) in 293T cells, immunoprecipitated with anti-His antibody, and immunoblotted with anti-Flag antibody. The structures of MyD88 and the deletion mutants and the NS5A binding region are indicated on the left. (C) Flag-MyD88 (left) or Flag-NS5A (middle) was coexpressed with IRAK-1–Myc or IRAK-4–Myc in 293T cells, immunoprecipitated with anti-Myc antibody, and immunoblotted with anti-Flag antibody. Flag-MyD88 and IRAK-1–Myc were coexpressed with Flag-NS5A in 293T cells, immunoprecipitated with anti-Myc antibody, and immunoblotted with anti-Flag antibody. The effect of the increase in Flag-NS5A expression on the interaction of MyD88 with IRAK-1 was examined by transfection with 0.1, 0.5, or 2 μg of Flag-NS5A expression plasmid (right).

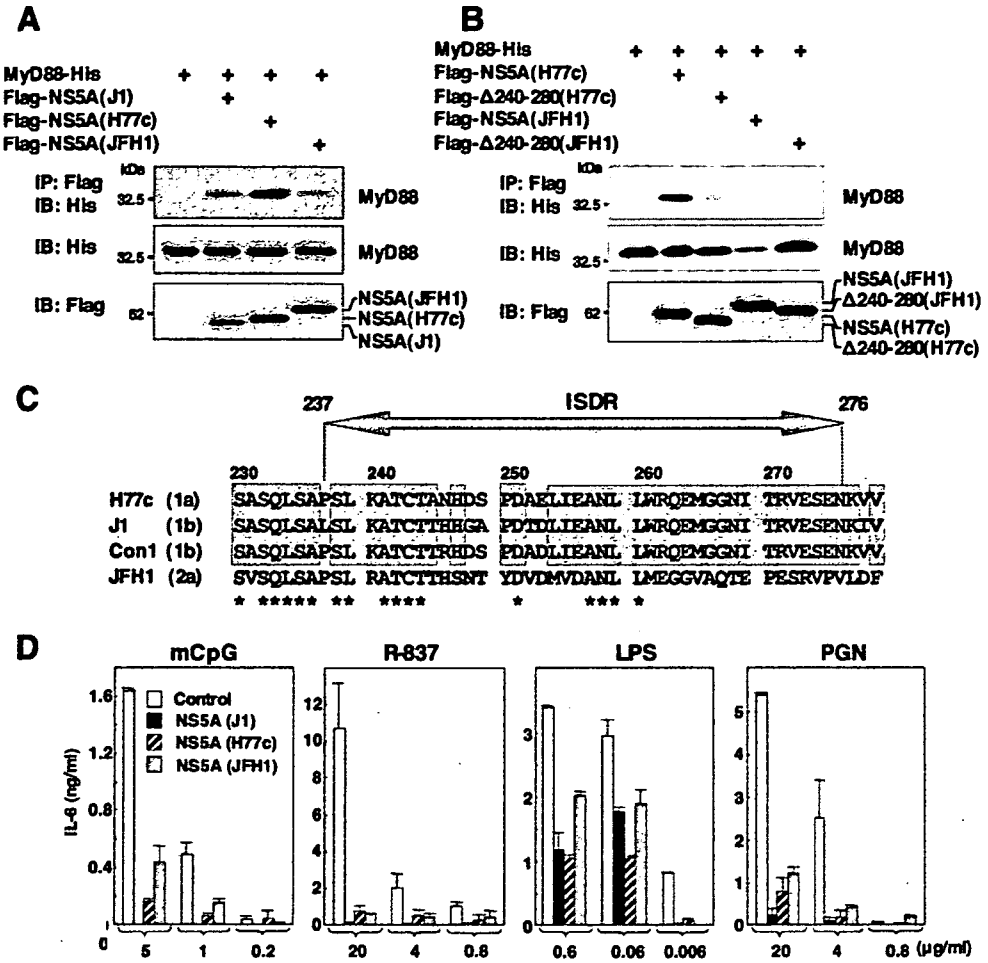

FIG. 7. NS5A of other genotypes also interacts with MyD88 and inhibits the TLR signaling pathway. (A) Flag-NS5As of other genotypes were coexpressed with MyD88-His in 293T cells, immunoprecipitated (IP) with anti-Flag antibody, and immunoblotted (IB) with anti-His antibody. (B) The wild type or a deletion mutant lacking amino acids 240 to 280 of Flag-NS5A of genotype 1a or 2a was coexpressed with MyD88-His in 293T cells, immunoprecipitated with anti-Flag antibody, and immunoblotted with anti-His antibody. (C) Amino acid sequences of ISDR and its adjacent region of strains H77c (genotype 1a), J1 (genotype 1b), Con1 (genotype 1b), and JFH1 (genotype 2a). The conserved amino acids among genotypes 1a and 1b are indicated by boxes. Conserved amino acids among all strains are indicated by asterisks. (D) Macrophage cell lines expressing NS5A of genotypes 1a (H77c), 1b (J1), and 2a (JFH1) were established. Cells were stimulated with the indicated amounts of mCpG, R-837, LPS, or PGN, and the production of IL-6 in the culture supernatants was determined by ELISA 24 h after stimulation. Data are shown as the means ± SD.

of IRAK-1 and MyD88 decreased in accord with the increasing NS5A expression complex (Fig. 6C, right), suggesting that the expression of NS5A may interfere with the TLR-MyD88-dependent signaling pathway through the inhibition of the recruitment of IRAK-1 to MyD88.

NS5A of other genotypes also interacts with MyD88 and inhibits the TLR signaling pathway. To determine the interaction of MyD88 with NS5A of other genotypes, Flag-tagged NS5A of genotype 1a (H77c) or 2a (JFH1) was coexpressed with His-tagged MyD88 in 293T cells. MyD88 was coprecipitated with the NS5As of genotypes 1a and 2a, although it should be noted that the interaction between the MyD88 and NS5A of genotype 2a was weaker than that of the other genotypes (Fig. 7A). To determine the region of the NS5As of genotype 1a or 2a responsible for the interaction with MyD88, N-terminal Flag-tagged NS5As of genotype 1a or 2a deletion mutants lacking amino acids 240 to 280 (Δ240–280) were constructed, and their interaction with MyD88 was examined. Mutational analyses revealed that amino acid residues 240 to 280 of the NS5As of genotypes 1a and 2a were also required for the interaction with MyD88 (Fig. 7B). Amino acid alignment of the ISDRs of genotypes 1a, 1b, and 2a revealed that the region of genotype 2a was less conserved than those of the other genotypes (Fig. 7C).

To determine the effect of NS5A expression of other genotypes on the TLR signaling pathway, we established macrophage cell lines expressing NS5A of each genotype. NS5A expression for all genotypes was found to inhibit IL-6 production after stimulation with mCpG, R-837, LPS, or PGN (Fig. 7D). Although the association of NS5A of genotype 2a to MyD88 was weaker than that of other genotypes, the expression of genotype 2a NS5A in macrophage cells exhibited com-

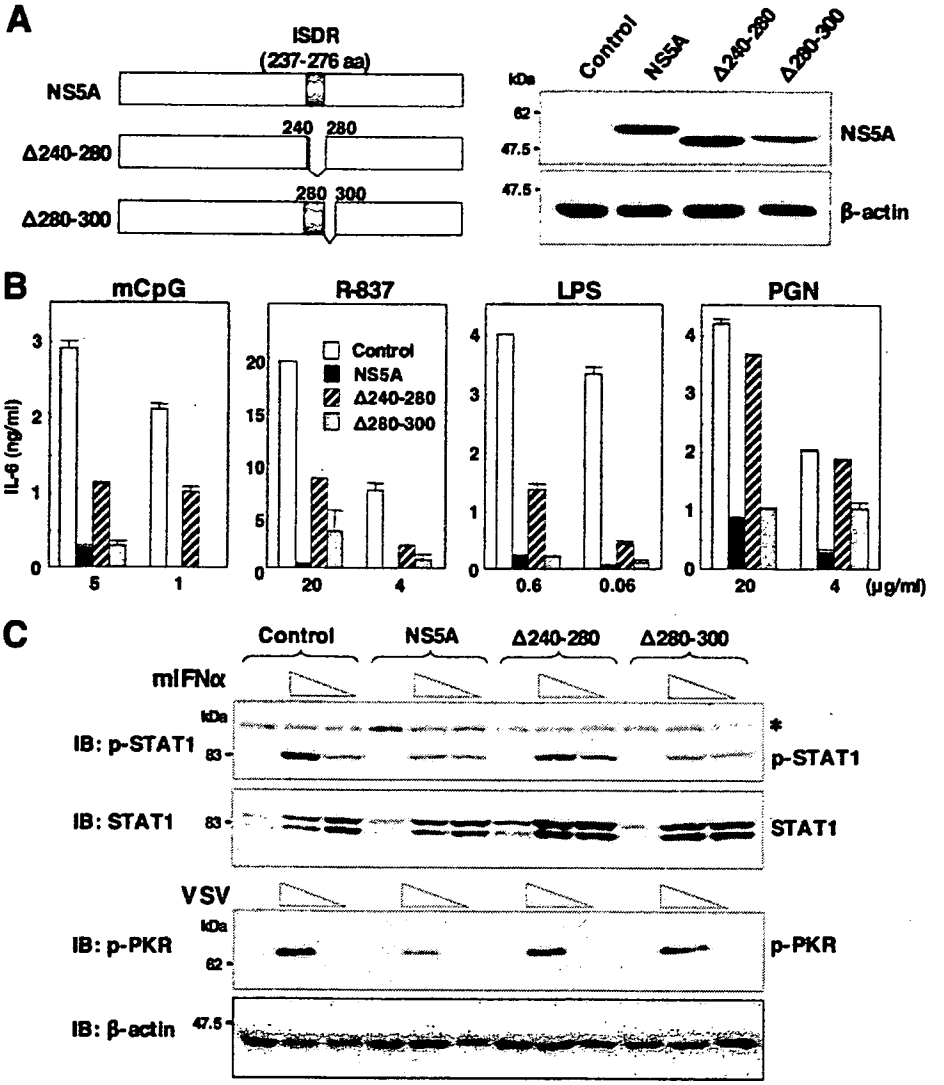

FIG. 8. ISDR in NS5A participates in the inhibition of the MyD88-dependent signaling pathway. (A) Structures of NS5A mutants lacking amino acid residues 240 to 280, in which the ISDR/MyD88-interacting region is located (Δ240–280), and lacking amino acid residues 280 to 300 (Δ280–300) (left). Immunoblot analyses of cells expressing wild-type or mutant NS5A (right) are shown. (B) Cells expressing wild-type or mutant NS5A were stimulated with the indicated amounts of mCpG, R-837, LPS, or PGN, and the production of IL-6 in the culture supernatants was determined by ELISA 24 h after stimulation. Data are shown as the means ± SD. (C) Phosphorylation of STAT1 or PKR in response to treatment with murine IFN-α or infection with VSV. The cell lines were stimulated with two doses of murine IFN-α (2×10^3 and 2×10^2 units/ml) or VSV (2×10^7 and 2×10^6 PFU/ml). After 24 h of stimulation, cell extracts were immunoblotted (IB) with specific antibodies. Phosphorylated STAT1 and PKR and the total amounts of STAT1 and β-actin were determined. The asterisk indicates nonspecific bands.

parable inhibition of IL-6 production in response to stimulation by various TLR ligands with those of genotypes 1b and 1a. These results suggest that NS5As of genotypes 1a, 1b, and 2a interact with MyD88 and inhibit the TLR signaling pathway in macrophage cell lines.

ISDR participates in the inhibition of the MyD88-dependent signaling pathway by NS5A. To further confirm the inhibitory effect of NS5A on the TLR signaling pathway, we established macrophage cell lines stably expressing an NS5A mutant lacking the ISDR/MyD88 binding region (Δ240–280) or lacking a region dispensable for the interaction with MyD88 (Δ280–300) (Fig. 8A). The inhibitory effect of TLR signaling in response to stimulation with mCpG, R-837, LPS, or PGN by NS5A was partially restored in the cell line expressing the NS5A lacking the ISDR (Δ240–280), and comparable inhibition was observed in the cell line expressing the NS5A deletion mutant retaining the ISDR (Δ280–300) (Fig. 8B). These results suggest that the interaction of NS5A with MyD88 through the ISDR is responsible for the disruption of the TLR-MyD88-dependent signaling pathway due to the expression of NS5A in macrophage cells. Partial recovery of the TLR signaling pathway by the expression of the NS5A mutant lacking the ISDR suggests the involvement of other inhibitory mechanisms by NS5A.

Previous reports suggested that the ISDR of NS5A participates in conferring IFN sensitivity (10) and in an interaction with PKR (13). To determine the effect of the interaction of MyD88 with NS5A through the ISDR on the IFN signaling pathway, we examined the phosphorylation of STAT1 and PKR in response to treatment with murine IFN-α and infection with VSV. The expression of wild-type NS5A and the Δ280–300 mutant but not the Δ240–280 mutant reduced the phosphorylation of STAT1 in response to IFN-α treatment (Fig. 8C, top), suggesting that the ISDR/MyD88 binding region in NS5A is involved in the IFN signaling pathway. Although cells expressing wild-type NS5A reduced PKR phosphorylation, those expressing mutant NS5A (Δ240–280 or Δ280–300) did not inhibit PKR phosphorylation upon infection with VSV (Fig. 8C, bottom), which is consistent with the previous observation that the 66 ISDR-inclusive amino acid residues (amino acids 237 to 302) are required for interactions with PKR (13). These results suggest that the expression of HCV NS5A in macrophage cells counteracts the IFN signaling pathway through the repression of STAT1 and PKR due to the interaction with ISDR and its adjacent region.

DISCUSSION

The majority of HCV-infected individuals become chronic carriers; however, the mechanism of progression to chronicity remains unclear. Among HCV proteins, NS3 has been shown to be immunodominant, and T cells that are reactive to NS3 have been suggested to play a crucial role in viral clearance, while HCV core protein is immunosuppressive (8). Treatment of immature DCs with core or NS3 protein inhibited DC differentiation, and DCs transduced to express core or E1 protein exhibited poor allogeneic T-cell responses (43). The immunosuppressive potential of HCV proteins has been implicated as a mechanism of the functional subversion of T cells, natural killer (NK) cells, and DCs. The association of HCV core protein with the globular domain of the C1q receptor on T cells down-regulates T-cell proliferation and IL-2 production (25). Additionally, the HCV E2 protein displays a high affinity for the tetraspanin cell surface molecule human CD81, which is one of the candidates for an HCV entry receptor (40), and E2 cross-linking with cell surface human CD81 impairs the activation of NK cells (7, 52).

In the present study, we established macrophage cell lines stably expressing HCV proteins and examined the effects of viral proteins on TLR function. The expression of the NS5A protein specifically inhibits TLR-MyD88-induced signaling by associating with the death domain of MyD88 through the ISDR spanning amino acid residues 240 to 280 in macrophage cells. HCV NS5A is a phosphoprotein that appears to possess multiple and diverse functions in viral replication, IFN resistance, and pathogenesis (34). Mutation in the ISDR has been suggested to correlate with the responsiveness of patients chronically infected with HCV genotype 1b to IFN treatment (10). Furthermore, NS5A has been shown to rescue virus replication in IFN-treated cell cultures (41) and to inhibit the antiviral activity of IFN by binding to PKR through the ISDR and its adjacent region (amino acids 237 to 302) (13, 14). However, controversial observations that the ISDR sequence variation does not account for differences in IFN sensitivity in patients (9) and also in an HCV subgenomic RNA replicon system (15) have been made. Moreover, the expression of NS5A or the entire HCV polyprotein has been reported to counteract the antiviral effect of IFN in a PKR- and ISDR-independent manner (12). Therefore, the possibility remains that a molecule other than PKR may be involved in the NS5A-mediated inhibition of IFN (50). Restoration of the phosphorylation of STAT1 in cells expressing a deletion mutant lacking ISDR in response to IFN-α and that of PKR phosphorylation upon infection with VSV in cells expressing NS5A mutants lacking amino acid residues 240 to 280 (ISDR) or 280 to 300 may support the hypothesis that the ISDR and the adjacent region are involved in IFN sensitivity. Thus, the ISDR may participate not only in conferring IFN resistance but also in disrupting TLR-MyD88 signaling pathways in macrophage cells.

Several viral proteins have been shown to counteract TLRs and their downstream signaling cascade. The vaccinia virus A46R protein contains a Toll/IL-1 receptor domain that interacts with multiple Toll/IL-1 receptor-containing adaptor molecules, thereby inhibiting the activation of NF-κB and IRF3 (49). Measles virus and respiratory syncytial virus have been shown to inhibit the TLR7- and TLR9-dependent IFN-inducing pathways stimulated by R848 and CpG oligodeoxynucleotides in primary human pDCs (45). HCV NS3/4A has been shown to influence the functions of adaptor molecules mediating TLR-dependent and -independent signaling pathways, resulting in an impairment of the induction of IFN-β as well as the subsequent IFN-inducible genes (11). Recently, RIG-I and MDA5 have been identified as being cytoplasmic dsRNA detectors responding to viral RNAs and poly(I:C) in a TLR-independent manner and recruit IPS-1 as an adaptor molecule for signal transduction (24). The uncapped 5′-triphosphate RNA generated by viral polymerases was shown to be selectively recognized by RIG-I (18, 39). In this study, we could demonstrate that the invasion of VSV and poly(I:C) into RAW cell lines is preferentially recognized by RIG-1–IPS-1- and TLR3-TRIF-dependent signaling pathways, respectively, and that the expression of HCV NS3/4A protease selectively inhibits cytokine production upon infection with VSV through the cleavage of IPS-1. Therefore, it is feasible that the expression of NS5A and NS3/4A proteins in macrophage cells may disrupt TLR-dependent and -independent signaling pathways, respectively. However, the mechanism for the inhibition of the TLR signaling pathway in the macrophage cells by the expression of NS3 or NS4B remains unclear.

Although there have been reports suggesting a lack of DC dysfunction in both chimpanzees and humans chronically infected with HCV (26, 32), direct infection of DCs with HCV may be a plausible mechanism for the dysfunction of DCs in patients with chronic HCV infection (4, 21). Indeed, the HCV genome has been detected in DCs by PCR (4), and HCV was detected in a monocyte/macrophage subpopulation of peripheral blood mononuclear cells from patients with chronic HCV infection (5). Further experiments are needed to exclude the possibility of contamination of viral RNA in blood samples. Pseudotype VSV-bearing chimeric HCV E1 and E2 proteins have been shown to infect immature myeloid DCs isolated from healthy donors through interactions with lectins in a Ca-independent manner (20). Recently, the in vitro replication

of the HCV JFH1 clone of genotype 2a isolated from an HCV-infected patient who developed fulminant hepatitis was reported (31, 54, 59). However, in vitro replication was limited in the combination of HCV clones derived from strain JFH1 and certain human hepatoma cell lines, and a robust cell culture of genotypes 1a and 1b, the most prevalent viruses in the world and resistant to IFN therapy, has not yet been successful except for a cell culture system for strain H77-S (genotype 1a) in which infectivity was significantly lower than that of the JFH1 clone (56). The establishment of a robust and reliable in vitro replication system for various HCV isolates is essential to determine the role of HCV infection in the modulation of TLR function in immunocompetent cells.

In conclusion, we have shown that the expression of the HCV nonstructural protein NS3, NS3/4A, NS4B, or NS5A impairs the activation of TLR signaling pathways in immunocompetent cells. Furthermore, the NS5A protein was shown to inhibit the TLR-MyD88 signaling pathway by a direct interaction with the death domain of MyD88 through the ISDR. These findings suggest new aspects of virus-cell interactions that may be explored to develop a greater understand of the mechanisms of escape of HCV from the host immune surveillance system and the establishment of persistent infection. However, it remains to be proven whether the results obtained using murine macrophage cell lines are applicable to immunocompetent cells in patients with HCV infection.

ACKNOWLEDGMENTS

We gratefully thank H. Murase for her secretarial work.

This work was supported in part by grants-in-aid from the Ministry of Health, Labor, and Welfare; the Ministry of Education, Culture, Sports, Science, and Technology; the 21st Century Center of Excellence Program; and the Foundation for Biomedical Research and Innovation.

REFERENCES

1. **Aizaki, H., Y. Aoki, T. Harada, K. Ishii, T. Suzuki, S. Nagamori, G. Toda, Y. Matsuura, and T. Miyamura.** 1998. Full-length complementary DNA of hepatitis C virus genome from an infectious blood sample. Hepatology **27:** 621–627.
2. **Akira, S., and K. Takeda.** 2004. Toll-like receptor signalling. Nat. Rev. Immunol. **4:**499–511.
3. **Applequist, S. E., R. P. Wallin, and H. G. Ljunggren.** 2002. Variable expression of Toll-like receptor in murine innate and adaptive immune cell lines. Int. Immunol. **14:**1065–1074.
4. **Bain, C., A. Fatmi, F. Zoulim, J. P. Zarski, C. Trepo, and G. Inchauspe.** 2001. Impaired allostimulatory function of dendritic cells in chronic hepatitis C infection. Gastroenterology **120:**512–524.
5. **Bouffard, P., P. H. Hayashi, R. Acevedo, N. Levy, and J. B. Zeldis.** 1992. Hepatitis C virus is detected in a monocyte/macrophage subpopulation of peripheral blood mononuclear cells of infected patients. J. Infect. Dis. **166:** 1276–1280.
6. **Cerny, A., J. G. McHutchison, C. Pasquinelli, M. E. Brown, M. A. Brothers, B. Grabscheid, P. Fowler, M. Houghton, and F. V. Chisari.** 1995. Cytotoxic T lymphocyte response to hepatitis C virus-derived peptides containing the HLA A2.1 binding motif. J. Clin. Investig. **95:**521–530.
7. **Crotta, S., A. Stilla, A. Wack, A. D'Andrea, S. Nuti, U. D'Oro, M. Mosca, F. Filliponi, R. M. Brunetto, F. Bonino, S. Abrignani, and N. M. Valiante.** 2002. Inhibition of natural killer cells through engagement of CD81 by the major hepatitis C virus envelope protein. J. Exp. Med. **195:**35–41.
8. **Dolganiuc, A., K. Kodys, A. Kopasz, C. Marshall, T. Do, L. Romics, Jr., P. Mandrekar, M. Zapp, and G. Szabo.** 2003. Hepatitis C virus core and nonstructural protein 3 proteins induce pro- and anti-inflammatory cytokines and inhibit dendritic cell differentiation. J. Immunol. **170:**5615–5624.
9. **Duverlie, G., H. Khorsi, S. Castelain, O. Jaillon, J. Izopet, F. Lunel, F. Eb, F. Penin, and C. Wychowski.** 1998. Sequence analysis of the NS5A protein of European hepatitis C virus 1b isolates and relation to interferon sensitivity. J. Gen. Virol. **79:**1373–1381.
10. **Enomoto, N., I. Sakuma, Y. Asahina, M. Kurosaki, T. Murakami, C. Yamamoto, N. Izumi, F. Marumo, and C. Sato.** 1995. Comparison of full-length sequences of interferon-sensitive and resistant hepatitis C virus 1b. Sensitivity to interferon is conferred by amino acid substitutions in the NS5A region. J. Clin. Investig. **96:**224–230.
11. **Foy, E., K. Li, C. Wang, R. Sumpter, Jr., M. Ikeda, S. M. Lemon, and M. Gale, Jr.** 2003. Regulation of interferon regulatory factor-3 by the hepatitis C virus serine protease. Science **300:**1145–1148.
12. **Francois, C., G. Duverlie, D. Rebouillat, H. Khorsi, S. Castelain, H. E. Blum, A. Gatignol, C. Wychowski, D. Moradpour, and E. F. Meurs.** 2000. Expression of hepatitis C virus proteins interferes with the antiviral action of interferon independently of PKR-mediated control of protein synthesis. J. Virol. **74:**5587–5596.
13. **Gale, M., Jr., C. M. Blakely, B. Kwieciszewski, S. L. Tan, M. Dossett, N. M. Tang, M. J. Korth, S. J. Polyak, D. R. Gretch, and M. G. Katze.** 1998. Control of PKR protein kinase by hepatitis C virus nonstructural 5A protein: molecular mechanisms of kinase regulation. Mol. Cell. Biol. **18:**5208–5218.
14. **Gale, M. J., Jr., M. J. Korth, N. M. Tang, S. L. Tan, D. A. Hopkins, T. E. Dever, S. J. Polyak, D. R. Gretch, and M. G. Katze.** 1997. Evidence that hepatitis C virus resistance to interferon is mediated through repression of the PKR protein kinase by the nonstructural 5A protein. Virology **230:**217–227.
15. **Guo, J. T., V. V. Bichko, and C. Seeger.** 2001. Effect of alpha interferon on the hepatitis C virus replicon. J. Virol. **75:**8516–8523.
16. **Hamamoto, I., Y. Nishimura, T. Okamoto, H. Aizaki, M. Liu, Y. Mori, T. Abe, T. Suzuki, M. M. Lai, T. Miyamura, K. Moriishi, and Y. Matsuura.** 2005. Human VAP-B is involved in hepatitis C virus replication through interaction with NS5A and NS5B. J. Virol. **79:**13473–13482.
17. **Honda, K., H. Yanai, T. Mizutani, H. Negishi, N. Shimada, N. Suzuki, Y. Ohba, A. Takaoka, W. C. Yeh, and T. Taniguchi.** 2004. Role of a transductional-transcriptional processor complex involving MyD88 and IRF-7 in Toll-like receptor signaling. Proc. Natl. Acad. Sci. USA **101:**15416–15421.
18. **Hornung, V., J. Ellegast, S. Kim, K. Brzozka, A. Jung, H. Kato, H. Poeck, S. Akira, K. K. Conzelmann, M. Schlee, S. Endres, and G. Hartmann.** 2006. 5′-Triphosphate RNA is the ligand for RIG-I. Science **314:**994–997.
19. **Jayakar, H. R., and M. A. Whitt.** 2002. Identification of two additional translation products from the matrix (M) gene that contribute to vesicular stomatitis virus cytopathology. J. Virol. **76:**8011–8018.
20. **Kaimori, A., T. Kanto, C. K. Limn, Y. Komoda, C. Oki, M. Inoue, H. Miyatake, I. Itose, M. Sakakibara, T. Yakushijin, T. Takehara, Y. Matsuura, and N. Hayashi.** 2004. Pseudotype hepatitis C virus enters immature myeloid dendritic cells through the interaction with lectin. Virology **324:**74–83.
21. **Kanto, T., N. Hayashi, T. Takehara, T. Tatsumi, N. Kuzushita, A. Ito, Y. Sasaki, A. Kasahara, and M. Hori.** 1999. Impaired allostimulatory capacity of peripheral blood dendritic cells recovered from hepatitis C virus-infected individuals. J. Immunol. **162:**5584–5591.
22. **Kawai, T., and S. Akira.** 2006. Innate immune recognition of viral infection. Nat. Immunol. **7:**131–137.
23. **Kawai, T., S. Sato, K. J. Ishii, C. Coban, H. Hemmi, M. Yamamoto, K. Terai, M. Matsuda, J. Inoue, S. Uematsu, O. Takeuchi, and S. Akira.** 2004. Interferon-alpha induction through Toll-like receptors involves a direct interaction of IRF7 with MyD88 and TRAF6. Nat. Immunol. **5:**1061–1068.
24. **Kawai, T., K. Takahashi, S. Sato, C. Coban, H. Kumar, H. Kato, K. J. Ishii, O. Takeuchi, and S. Akira.** 2005. IPS-1, an adaptor triggering RIG-I- and Mda5-mediated type I interferon induction. Nat. Immunol. **6:**981–988.
25. **Kittlesen, D. J., K. A. Chianese-Bullock, Z. Q. Yao, T. J. Braciale, and Y. S. Hahn.** 2000. Interaction between complement receptor gC1qR and hepatitis C virus core protein inhibits T-lymphocyte proliferation. J. Clin. Investig. **106:**1239–1249.
26. **Larsson, M., E. Babcock, A. Grakoui, N. Shoukry, G. Lauer, C. Rice, C. Walker, and N. Bhardwaj.** 2004. Lack of phenotypic and functional impairment in dendritic cells from chimpanzees chronically infected with hepatitis C virus. J. Virol. **78:**6151–6161.
27. **Lechner, F., D. K. Wong, P. R. Dunbar, R. Chapman, R. T. Chung, P. Dohrenwend, G. Robbins, R. Phillips, P. Klenerman, and B. D. Walker.** 2000. Analysis of successful immune responses in persons infected with hepatitis C virus. J. Exp. Med. **191:**1499–1512.
28. **Li, K., E. Foy, J. C. Ferreon, M. Nakamura, A. C. Ferreon, M. Ikeda, S. C. Ray, M. Gale, Jr., and S. M. Lemon.** 2005. Immune evasion by hepatitis C virus NS3/4A protease-mediated cleavage of the Toll-like receptor 3 adaptor protein TRIF. Proc. Natl. Acad. Sci. USA **102:**2992–2997.
29. **Li, X. D., L. Sun, R. B. Seth, G. Pineda, and Z. J. Chen.** 2005. Hepatitis C virus protease NS3/4A cleaves mitochondrial antiviral signaling protein off the mitochondria to evade innate immunity. Proc. Natl. Acad. Sci. USA **102:**17717–17722.
30. **Lin, R., J. Lacoste, P. Nakhaei, Q. Sun, L. Yang, S. Paz, P. Wilkinson, I. Julkunen, D. Vitour, E. Meurs, and J. Hiscott.** 2006. Dissociation of a MAVS/IPS-1/VISA/Cardif-IKKε molecular complex from the mitochondrial outer membrane by hepatitis C virus NS3-4A proteolytic cleavage. J. Virol. **80:**6072–6083.
31. **Lindenbach, B. D., M. J. Evans, A. J. Syder, B. Wolk, T. L. Tellinghuisen, C. C. Liu, T. Maruyama, R. O. Hynes, D. R. Burton, J. A. McKeating, and C. M. Rice.** 2005. Complete replication of hepatitis C virus in cell culture. Science **309:**623–626.

32. **Longman, R. S., A. H. Talal, I. M. Jacobson, M. L. Albert, and C. M. Rice.** 2004. Presence of functional dendritic cells in patients chronically infected with hepatitis C virus. Blood **103**:1026–1029.
33. **Loo, Y. M., D. M. Owen, K. Li, A. K. Erickson, C. L. Johnson, P. M. Fish, D. S. Carney, T. Wang, H. Ishida, M. Yoneyama, T. Fujita, T. Saito, W. M. Lee, C. H. Hagedorn, D. T. Lau, S. A. Weinman, S. M. Lemon, and M. Gale, Jr.** 2006. Viral and therapeutic control of IFN-beta promoter stimulator 1 during hepatitis C virus infection. Proc. Natl. Acad. Sci. USA **103**:6001–6006.
34. **Macdonald, A., and M. Harris.** 2004. Hepatitis C virus NS5A: tales of a promiscuous protein. J. Gen. Virol. **85**:2485–2502.
35. **Meylan, E., J. Curran, K. Hofmann, D. Moradpour, M. Binder, R. Bartenschlager, and J. Tschopp.** 2005. Cardif is an adaptor protein in the RIG-I antiviral pathway and is targeted by hepatitis C virus. Nature **437**:1167–1172.
36. **Moriishi, K., and Y. Matsuura.** 2003. Mechanisms of hepatitis C virus infection. Antivir. Chem. Chemother. **14**:285–297.
37. **Niwa, H., K. Yamamura, and J. Miyazaki.** 1991. Efficient selection for high-expression transfectants with a novel eukaryotic vector. Gene **108**:193–199.
38. **Okamoto, K., K. Moriishi, T. Miyamura, and Y. Matsuura.** 2004. Intramembrane proteolysis and endoplasmic reticulum retention of hepatitis C virus core protein. J. Virol. **78**:6370–6380.
39. **Pichlmair, A., O. Schulz, C. P. Tan, T. I. Naslund, P. Liljestrom, F. Weber, and C. Reis e Sousa.** 2006. RIG-I-mediated antiviral responses to single-stranded RNA bearing 5′-phosphates. Science **314**:997–1001.
40. **Pileri, P., Y. Uematsu, S. Campagnoli, G. Galli, F. Falugi, R. Petracca, A. J. Weiner, M. Houghton, D. Rosa, G. Grandi, and S. Abrignani.** 1998. Binding of hepatitis C virus to CD81. Science **282**:938–941.
41. **Polyak, S. J., D. M. Paschal, S. McArdle, M. J. Gale, Jr., D. Moradpour, and D. R. Gretch.** 1999. Characterization of the effects of hepatitis C virus nonstructural 5A protein expression in human cell lines and on interferon-sensitive virus replication. Hepatology **29**:1262–1271.
42. **Reis e Sousa, C.** 2004. Toll-like receptors and dendritic cells: for whom the bug tolls. Semin. Immunol. **16**:27–34.
43. **Sarobe, P., J. J. Lasarte, A. Zabaleta, L. Arribillaga, A. Arina, I. Melero, F. Borras-Cuesta, and J. Prieto.** 2003. Hepatitis C virus structural proteins impair dendritic cell maturation and inhibit in vivo induction of cellular immune responses. J. Virol. **77**:10862–10871.
44. **Sasai, M., H. Oshiumi, M. Matsumoto, N. Inoue, F. Fujita, M. Nakanishi, and T. Seya.** 2005. Cutting edge: NF-kappaB-activating kinase-associated protein 1 participates in TLR3/Toll-IL-1 homology domain-containing adapter molecule-1-mediated IFN regulatory factor 3 activation. J. Immunol. **174**:27–30.
45. **Schlender, J., V. Hornung, S. Finke, M. Gunthner-Biller, S. Marozin, K. Brzozka, S. Moghim, S. Endres, G. Hartmann, and K. K. Conzelmann.** 2005. Inhibition of Toll-like receptor 7- and 9-mediated alpha/beta interferon production in human plasmacytoid dendritic cells by respiratory syncytial virus and measles virus. J. Virol. **79**:5507–5515.
46. **Seth, R. B., L. Sun, C. K. Ea, and Z. J. Chen.** 2005. Identification and characterization of MAVS, a mitochondrial antiviral signaling protein that activates NF-kappaB and IRF 3. Cell **122**:669–682.
47. **Shi, S. T., S. J. Polyak, H. Tu, D. R. Taylor, D. R. Gretch, and M. M. Lai.** 2002. Hepatitis C virus NS5A colocalizes with the core protein on lipid droplets and interacts with apolipoproteins. Virology **292**:198–210.
48. **Shoukry, N. H., A. Grakoui, M. Houghton, D. Y. Chien, J. Ghrayeb, K. A. Reimann, and C. M. Walker.** 2003. Memory CD8+ T cells are required for protection from persistent hepatitis C virus infection. J. Exp. Med. **197**:1645–1655.
49. **Stack, J., I. R. Haga, M. Schroder, N. W. Bartlett, G. Maloney, P. C. Reading, K. A. Fitzgerald, G. L. Smith, and A. G. Bowie.** 2005. Vaccinia virus protein A46R targets multiple Toll-like-interleukin-1 receptor adaptors and contributes to virulence. J. Exp. Med. **201**:1007–1018.
50. **Taguchi, T., M. Nagano-Fujii, M. Akutsu, H. Kadoya, S. Ohgimoto, S. Ishido, and H. Hotta.** 2004. Hepatitis C virus NS5A protein interacts with 2′,5′-oligoadenylate synthetase and inhibits antiviral activity of IFN in an IFN sensitivity-determining region-independent manner. J. Gen. Virol. **85**:959–969.
51. **Thimme, R., D. Oldach, K. M. Chang, C. Steiger, S. C. Ray, and F. V. Chisari.** 2001. Determinants of viral clearance and persistence during acute hepatitis C virus infection. J. Exp. Med. **194**:1395–1406.
52. **Tseng, C. T., and G. R. Klimpel.** 2002. Binding of the hepatitis C virus envelope protein E2 to CD81 inhibits natural killer cell functions. J. Exp. Med. **195**:43–49.
53. **Uematsu, S., S. Sato, M. Yamamoto, T. Hirotani, H. Kato, F. Takeshita, M. Matsuda, C. Coban, K. J. Ishii, T. Kawai, O. Takeuchi, and S. Akira.** 2005. Interleukin-1 receptor-associated kinase-1 plays an essential role for Toll-like receptor (TLR)7- and TLR9-mediated interferon-α induction. J. Exp. Med. **201**:915–923.
54. **Wakita, T., T. Pietschmann, T. Kato, T. Date, M. Miyamoto, Z. Zhao, K. Murthy, A. Habermann, H. G. Krausslich, M. Mizokami, R. Bartenschlager, and T. J. Liang.** 2005. Production of infectious hepatitis C virus in tissue culture from a cloned viral genome. Nat. Med. **11**:791–796.
55. **Xu, L. G., Y. Y. Wang, K. J. Han, L. Y. Li, Z. Zhai, and H. B. Shu.** 2005. VISA is an adapter protein required for virus-triggered IFN-beta signaling. Mol. Cell **19**:727–740.
56. **Yi, M., R. A. Villanueva, D. L. Thomas, T. Wakita, and S. M. Lemon.** 2006. Production of infectious genotype 1a hepatitis C virus (Hutchinson strain) in cultured human hepatoma cells. Proc. Natl. Acad. Sci. USA **103**:2310–2315.
57. **Yoneyama, M., M. Kikuchi, K. Matsumoto, T. Imaizumi, M. Miyagishi, K. Taira, E. Foy, Y. M. Loo, M. Gale, Jr., S. Akira, S. Yonehara, A. Kato, and T. Fujita.** 2005. Shared and unique functions of the DExD/H-box helicases RIG-I, MDA5, and LGP2 in antiviral innate immunity. J. Immunol. **175**:2851–2858.
58. **Yoneyama, M., M. Kikuchi, T. Natsukawa, N. Shinobu, T. Imaizumi, M. Miyagishi, K. Taira, S. Akira, and T. Fujita.** 2004. The RNA helicase RIG-I has an essential function in double-stranded RNA-induced innate antiviral responses. Nat. Immunol. **5**:730–737.
59. **Zhong, J., P. Gastaminza, G. Cheng, S. Kapadia, T. Kato, D. R. Burton, S. F. Wieland, S. L. Uprichard, T. Wakita, and F. V. Chisari.** 2005. Robust hepatitis C virus infection in vitro. Proc. Natl. Acad. Sci. USA **102**:9294–9299.

JOURNAL OF VIROLOGY, Aug. 2007, p. 8477–8487
0022-538X/07/$08.00+0 doi:10.1128/JVI.00477-07

Vol. 81, No. 16

Processing of Capsid Protein by Cathepsin L Plays a Crucial Role in Replication of Japanese Encephalitis Virus in Neural and Macrophage Cells[▽]

Yoshio Mori, Tetsuo Yamashita, Yoshinori Tanaka, Yoshimi Tsuda,† Takayuki Abe, Kohji Moriishi, and Yoshiharu Matsuura*

Department of Molecular Virology, Research Institute for Microbial Diseases, Osaka University, Osaka, Japan

Received 6 March 2007/Accepted 25 May 2007

The flavivirus capsid protein not only is a component of nucleocapsids but also plays a role in viral replication. In this study, we found a small capsid protein in cells infected with Japanese encephalitis virus (JEV) but not in the viral particles. The small capsid protein was shown to be generated by processing with host cysteine protease cathepsin L. An in vitro cleavage assay revealed that cathepsin L cleaves the capsid protein between amino acid residues Lys^{18} and Arg^{19}, which are well conserved among the mosquito-borne flaviviruses. A mutant JEV resistant to the cleavage of the capsid protein by cathepsin L was generated from an infectious cDNA clone of JEV by introducing a substitution in the cleavage site. The mutant JEV exhibited growth kinetics similar to those of the wild-type JEV in monkey (Vero), mosquito (C6/36), and porcine (PK15) cell lines, whereas replication of the mutant JEV in mouse macrophage (RAW264.7) and neuroblastoma (N18) cells was impaired. Furthermore, the neurovirulence and neuroinvasiveness of the mutant JEV to mice were lower than those of the wild-type JEV. These results suggest that the processing of the JEV capsid protein by cathepsin L plays a crucial role in the replication of JEV in neural and macrophage cells, which leads to the pathogenesis of JEV infection.

The genus *Flavivirus* within the family *Flaviviridae* comprises over 70 viruses, many of which are predominantly arthropod-borne viruses, such as Japanese encephalitis virus (JEV), West Nile virus (WNV), Murray Valley encephalitis virus (MVE), dengue virus (DEN), yellow fever virus (YFV), and tick-borne encephalitis virus (TBEV). They frequently cause significant morbidity and mortality in mammals and birds (5). JEV is distributed in the south and southeast regions of Asia and is kept in a zoonotic transmission cycle between pigs or birds and mosquitoes (5, 42, 45). JEV spreads to dead-end hosts, including humans, through the bite of JEV-infected mosquitoes and causes infection of the central nervous system with a high mortality rate (5, 45). JEV has a single-stranded positive-strand RNA genome of approximately 11 kb, which is capped at the 5′ end but lacks a 3′ polyadenine tail (24). The ability of the flaviviral genomic RNA to cyclize is crucial for viral replication (1, 14). Among mosquito-borne flaviviruses, two complementary cyclization sequences, mapped in the capsid protein-coding region and 3′ untranslated region (UTR), mediated the cyclization by RNA-RNA base pairing, together with a second pair of complementary sequences, named 5′ and 3′ upstream AUG regions (1, 10, 14, 19, 25). The genomic RNA includes a single large open reading frame, and a polyprotein translated at the endoplasmic reticulum (ER) membrane is cleaved co- and posttranslationally by host and viral proteases to yield three structural proteins, the capsid, precursor membrane (prM), and envelope (E) proteins, and at least seven nonstructural proteins, NS1, NS2A, NS2B, NS3, NS4A, NS4B, and NS5 (24).

Although the capsid protein has very little amino acid homology among flaviviruses—for example, the homologies of the capsid protein of JEV to those of WNV, DEN type 2 (DEN2), and TBEV were only 67%, 33%, and 25%, respectively—the structural properties, such as the hydrophobicity profile, abundance of basic amino acid residues, and secondary and tertiary structures, are well conserved (11, 18, 27). The flavivirus capsid protein commonly contains two hydrophobic sequences in the center and the carboxyl terminus. The latter serves as a signal sequence of prM. The signal/anchor sequence is cleaved off by the viral protease NS2B/3, and this cleavage is required for the subsequent liberation of the amino terminus of prM by the host signal peptidase (26, 43, 49). The mature capsid protein may be associated with the ER membrane through the central hydrophobic region (23, 29). Because the capsid protein has RNA-binding ability via the basic amino acid clusters at its amino and carboxyl termini, it is believed to bind to the genomic RNA to form a nucleocapsid (20). Unlike other envelope viruses, the nucleocapsid structures are rarely found in cells infected with flaviviruses (48), although the nucleocapsid of TBEV can assemble in vitro (21). Therefore, viral assembly is thought to be a coordinated process between the membrane-associated capsid protein and two envelope glycoproteins, prM and E, in the ER membrane.

In conflict with their roles as structural proteins, the capsid proteins of some flaviviruses are localized not only in the cytoplasm but also in the nuclei of the infected cells (4, 28, 32, 44, 46–48). We previously reported that the JEV capsid protein

* Corresponding author. Mailing address: Department of Molecular Virology, Research Institute for Microbial Diseases, Osaka University, 3-1 Yamada-oka, Suita, Osaka 565-0871, Japan. Phone: 81-6-6879-8340. Fax: 81-6-6879-8269. E-mail: matsuura@biken.osaka-u.ac.jp.
† Present address: Department of Disease Control, Graduate School of Veterinary Medicine, Hokkaido University, Sapporo 060-0818, Japan.
▽ Published ahead of print on 6 June 2007.

has also been detected in both the nucleoli and cytoplasm and that the mutant virus defective in the nuclear localization of capsid protein exhibited impaired viral growth in mammalian cells and neuroinvasiveness in mice (32). Furthermore, we have also reported that the nuclear and cytoplasmic localizations of the JEV capsid protein are dependent on binding to the host nucleolar protein B23 (46). It has been reported that, in addition to the JEV capsid protein, the WNV and DEN capsid proteins bind to several host proteins, such as Jab1, a component of the COP9 signalosome complex (34), the chaperone protein HSP70 (35), and the heterogenous nuclear ribonucleoprotein K (8), to regulate these functions. Recently, Clyde and Harris have shown that the small capsid protein isoform translated from the second AUG codon of the DEN genome by leaky scanning is important for viral replication (9). In this context, these properties of the flaviviral capsid proteins raised the possibility that they play some roles in viral growth as "nonstructural" proteins.

In this study, we detected a small capsid protein in JEV-infected cells, but not in the released viral particles. The small capsid protein has been shown to be generated by host protease cathepsin L. Cathepsin L was capable of cleaving the capsid protein between amino acid residues Lys^{18} and Arg^{19}. Furthermore, we have generated a mutant JEV carrying a capsid protein resistant to cleavage by cathepsin L. The characterization of this mutant JEV indicated that cleavage of the capsid protein by cathepsin L plays important roles in viral replication in mouse neuroblastoma and macrophage cells and in the pathogenesis of encephalitis in vivo. These results suggest a novel mechanism for JEV to adapt host cells by the processing of the capsid protein.

MATERIALS AND METHODS

Cells. The mammalian cell lines Vero (monkey kidney), 293T (human kidney), PK15 (pig kidney), RAW264.7 (mouse macrophage), and N18 (mouse neuroblastoma) were maintained in Dulbecco's modified Eagle's minimal essential medium (DMEM) supplemented with 10% fetal bovine serum (FBS). Mosquito cell line C6/36 (*Aedes albopictus*) was grown in Eagle's minimal essential medium supplemented with 10% FBS. Vero cell lines Vero/siNC and Vero/siCTSL, stably expressing the hairpin small interfering RNAs (siRNA) for the nonsense sequence and cathepsin L, respectively, were established by transfection with plasmids pSilencer/NC and pSilencer/CTSL (see below), respectively, and selected with DMEM containing 10% FBS and 50 μg/ml hygromycin B (Sigma, St. Louis, MO).

Plasmids. The cDNA for the capsid protein of JEV AT31 (amino acid residues 2 to 105) was amplified from pMWATG1 (54) by PCR using Ex-*Taq* (Takara, Shiga, Japan) and cloned between the FLAG and hemagglutinin (HA) tags in pcDNA3.1FlagHA (36). From this plasmid, the capsid cDNAs with or without FLAG and/or HA tags were amplified by PCR and subcloned into a mammalian expression vector pCAGPM (31) and designated pCAG/FLAG-JEC-HA, pCAG/FLAG-JEC, pCAG/JEC-HA, and pCAG/JEC. By the same procedure, the plasmids encoding FLAG- and HA-tagged DEN2 and DEN4 capsid proteins, pCAG/FLAG-DEN2C-HA and pCAG/FLAG-DEN4C-HA, were generated from the plasmids encoding the capsid proteins of DEN2 and DEN4, respectively (the kind gifts from F. Hasebe and M. Tadano, respectively). For mutational analyses of the amino acid residues from 14 to 23 (based on the JEV capsid protein sequence), a series of point mutants of the FLAG- and HA-tagged JEV capsid proteins were synthesized by PCR-based mutagenesis (17). All of the mutant genes, as well as the wild-type gene, were cloned into pCAGPM. The JEV capsid gene was cloned into pcDNA 3.1/myc-His (Invitrogen, Carlsbad, CA), and the cDNA encoding the JEV capsid protein fused with myc and His tags was amplified and cloned into bacterial expression vector pET32a (Merck Novagen, Darmstadt, Germany). The resulting plasmid was designated pET32/JECmycHis. The cDNAs of human cathepsins B and L were amplified from 293T cells by reverse transcription-PCR and cloned into pcDNA 3.1/myc-His. An enzymatically inactive mutation of cathepsin L in which Cys^{138} was replaced with Ala was generated by PCR-based mutagenesis. Expression vector pSilencer/CTSL, for a hairpin siRNA for African green monkey cathepsin L, was generated by annealing with synthesized nucleotides (sense, GAT CCG GCG ATG CAC AAC AGA TTA TTC AAG AGA TAA TCT GTT GTG CAT CGC CTT TTT TGG AAA; antisense, AGC TTT TCC AAA AAA GGC GAT GCA CAA CAG ATT ATC TCT TGA ATA ATC TGT TGT GCA TCG CCG) and insertion into the BamHI and HindIII sites of p*Silencer* 2.1 U6 hygro (Ambion Inc., Austin, TX). pSilencer/NC, encoding an siRNA with no homology to mammalian genes, was used as a negative control. pMWAT/L17A carrying replacements of cytosine at nucleotide 144 and thymine at nucleotide 145 with guanine and cytosine, respectively, in pMWATG1, an infectious cDNA clone of JEV, was constructed by PCR-based mutagenesis which results in the replacement of Leu^{17} in the capsid protein with Ala (see Fig. 5A). In addition, adenine-to-guanine and guanine-to-cytosine mutations were introduced into pMWATG1 and pMWAT/L17A at nucleotides 10865 and 10866 of the JEV gene, respectively. The resulting plasmids were named pMWAT/CSmt and pMWAT/L17ACSmt, respectively.

Viruses. The wild-type and L17A/CSmt JEVs were generated from plasmids pMWATG1 and pMWAT/L17ACSmt, respectively, by a method described previously (54). The infectivity of the viruses was determined by an immunostaining focus assay as described previously (32) and expressed in focus-forming units (FFU). The JEV particles were purified from the supernatant of the infected Vero cells as described previously with some modifications (32). Briefly, the virions were clarified by centrifugation at 6,000 × *g* for 30 min and precipitated with 10% polyethylene glycol (molecular mass, approximately 6,000 kDa). The precipitates were collected by centrifugation at 10,000 × *g* for 45 min and centrifuged at 147,000 × *g* for 20 h on a 20 to 60% sucrose gradient. The fractions ranging from 1.16 to 1.19 g/ml in gravity were used as the purified virion.

Antibodies. Anti-JEV capsid protein rabbit polyclonal antibody (PAb) was prepared as described previously (32). Monoclonal antibodies (MAbs) to JEV E (10B4) and NS3 proteins (34A1) were generous gifts from E. Konishi and K. Yasui, respectively. Anti-FLAG tag (M2) and anti-β-actin MAbs were purchased from Sigma. Anti-HA (HA11) and anti-myc tag (9E10) MAbs were purchased from Covance (Richmond, CA). An antinucleolin MAb (MS-3) was purchased from Santa Cruz Biotechnology (Santa Cruz, CA). Anti-PA28-alpha and anti-cathepsin L rabbit PAbs were purchased from Affinity Bioreagents (Golden, CO) and Merck Calbiochem (Darmstadt, Germany), respectively.

Infection, transfection, immunoblotting, and cell fractionation. A monolayer of Vero or N18 cells was infected at multiplicities of infection (MOI) of 5 and 10 with the wild-type and L17A/CSmt JEVs. Plasmids were transfected by *Trans*IT LT-1 (Mirus, Madison, WI) and Lipofectamine 2000 (Invitrogen) for Vero and 293T cells, respectively, according to the manufacturers' instructions. At 24 h after inoculation or transfection, cells were lysed on ice by Triton lysis buffer (20 mM Tris-HCl [pH 7.4], 135 mM NaCl, 1% Triton X-100, 10% glycerol) supplemented with a protease inhibitor cocktail (Biovision, Mountain View, CA) and subjected to sodium dodecyl sulfate-polyacrylamide gel electrophoresis (SDS-PAGE) and Western blotting as previously described (36, 46). JEV-infected cells were fractionated using a Nuclear/Cytosol Fractionation kit (Biovision).

Inhibition of capsid protein processing. E64d and CA074Me were purchased from the Peptide Institute (Osaka, Japan). Z-Phe-Tyr-(*tert*-butyl)-diazomethyl ketone (DMK) (Z-FY-DMK), Z-Val-Ala-Asp-fluoromethyl ketone (FMK) (Z-VAD-FMK), PD150606, and bafilomycin A1 were purchased from Merck Calbiochem. Chloroquine and ammonium chloride were obtained from Sigma and Nacalai Tesque (Kyoto, Japan), respectively. Chloroquine and ammonium chloride were dissolved in distilled water, and bafilomycin A1 was dissolved in ethanol. The other reagents were dissolved in dimethyl sulfoxide (DMSO). At 24 h after inoculation or transfection, cells were incubated with the culture medium containing each reagent or solvent for 8 h at 37°C and examined by immunoblotting. To determine the effects of CA074Me or FY-DMK on the cleavage of the capsid protein, cells transfected with pCAG/FLAG-JEC-HA were treated with the inhibitor for 8 h at 37°C. The ratios of the densities of the slower- and faster-migrating capsid proteins (C1 and C2, respectively) detected by immunoblotting were calculated by Multi Gauge software (Fujifilm, Tokyo, Japan). The relative cleavage values were determined as the C2 to C1 ratio in the presence of inhibitor/the C2 to C1 ratio in the absence of inhibitor. The inhibitory effects of CA074Me or Z-FY-DMK to cathepsins B and L were determined as described previously (7, 13) with some modifications. Briefly, Vero cells (2×10^5) were treated with CA074Me or Z-FY-DMK for 4 h at 37°C and lysed with 25 μl of acidic lysis buffer consisting of 100 mM sodium acetate (pH 5.0), 1 mM EDTA, 0.5% Triton X-100, 2 mM AEBSF [4-(2-aminoethyl)benzenesulfonyl fluoride] (Merck Calbiochem), 5 μg/ml aprotinin (Nacalai Tesque), 100 μM bestatin (Sigma), and 15 μM pepstatin (Peptide Institute). Insoluble materials

were sedimented in a microcentrifuge at 4°C. Ten microliters of each lysate was mixed with 90 μl of reaction buffer (100 mM sodium acetate [pH 5.0], 1 mM EDTA, 4 mM dithiothreitol, 2 mM AEBSF, 5 μg/ml aprotinin, 100 μM bestatin, 15 μM pepstatin). The resulting samples were mixed with 100 μl of cathepsin B-specific (100 μM Z-Arg-Arg-MCA [4-methylcoumaryl-7-amide; Peptide Institute], 0.1% Brij 35) (3) or cathepsin L-specific (100 μM $[Z\text{-Phe-Arg}]_2$-R110 [Molecular Probes, Eugene, OR], 0.1% Brij 35) (2) substrate solutions in a black 96-well plate (Corning, Corning, NY). After incubation for 30 min at room temperature, fluorescence was measured using a fluorescence multiwell plate reader (CytoFluor 4000 LX1; Applied Biosystems, Foster City, CA) with an excitation of 360 nm and an emission of 460 nm for cathepsin B and with an excitation of 485 nm and an emission of 460 nm for cathepsin L. The relative cleavage value in the absence of each inhibitor was defined as 1.

In vitro processing of the JEV capsid protein. The JEV capsid protein fused with thioredoxin and myc-His tags in the N and C termini, respectively, was purified using TALON metal affinity resin (Clontech, Mountain View, CA) from the lysate of *Escherichia coli* transformed by pET32/JECmycHis. The purified protein was dialyzed with acidic dialysis buffer (50 mM sodium acetate [pH 5.5], 1 mM EDTA) for 24 h at 4°C. The recombinant JEV capsid protein (33 μg [1 nmol]/100 μl) was incubated with 0.01 units (170 ng) of human cathepsin L (Merck Calbiochem) for 2 h at room temperature. According to the manufacturer's instructions, one unit is defined as an amount of the enzyme capable of hydrolyzing 1.0 μmol of Z-Phe-Arg-AMC (7-amino-4-methylcoumarin) per minute at 37°C. The resulting samples were subjected to SDS-PAGE and Western blotting using anti-myc MAb. The N-terminal peptide sequences of the cleaved capsid proteins were determined by the Edman degradation method at the APRO Life Science Institute (Tokushima, Japan).

Computer analyses of the flavivirus capsid genes. The amino acid sequences of the flavivirus capsid proteins were aligned with the software package GENETYX-MAC, version 12 (GENETYX, Tokyo, Japan). The GenBank accession numbers of the analyzed sequences are as follows: JEV AT31 strain, AB196923; MVE 1-51 strain, AF161266; WNV IS-98 STD1 strain, AF481864; DEN1 Singapore S275/90 strain, M87512; DEN2 New Guinea C strain, M29095; DEN3 H87 strain, M93130; DEN4 814669 strain, AF326573; YFV 17D strain, X03700. Nucleotides 135 to 152 and bases 10858 to 10875 in the 5′ and 3′ termini, respectively, connected by 8 X nucleotides alternative to bases 153 to 10857, of the wild-type and mutant JEV genomes were applied to GENETYX-MAC to predict RNA secondary structures with minimum free energy.

Growth kinetics of JEVs in vitro. Vero, C6/36, PK15, N18, RAW264.7, Vero/siNC, and Vero/siCTSL cells in 24-well plates (2×10^5) were infected with the wild-type or L17A/CSmt virus at an MOI of 5 for 1 h, washed three times with a medium to remove unbound viruses, and incubated with a medium supplemented with 5% FBS for a total duration of 72 h. To examine the effect of the cathepsin L inhibitor on virus growth, DMSO or 1 μM Z-FY-DMK was added to the culture medium over the incubation period (24 h). The culture supernatants were used for titration of infectious virus.

Mouse experiments. The pathogenicity of JEV to mice was determined as described previously (32). Briefly, 3-week-old female ICR mice were purchased from CLEA Japan (Osaka, Japan) and kept in special pathogen-free environments. Groups of 10 mice were intracerebrally inoculated with 30 μl of 10-fold-diluted solutions of wild-type or L17A/CSmt virus. The virus-diluting solution (DMEM) was administered to two mice as a control. The mice were observed for 2 weeks after inoculation to determine survival rates. The value of the 50% lethal dose (LD_{50}) of each virus was determined by the method by Reed and Müench (39). To examine viral growth in the brain, 100 FFU of the viruses were intracerebrally administered to the mice. At 3 and 5 days after inoculation, the mice were euthanized, and the brains were collected. The infectious titers in the homogenates of the brains were determined in Vero cells as described above. Groups of 10 mice were inoculated intraperitoneally with 1×10^6 FFU (100 μl) of the viruses. The mice were observed for 3 weeks after inoculation to determine survival rates.

RESULTS

JEV-infected cells contained a small capsid protein. Western blotting analyses of Vero cells infected with JEV revealed capsid proteins of 14 and 12 kDa, which were designated C1 and C2, respectively, in contrast to the purified viral particles, in which only C1 was detected (Fig. 1A), indicating that C1 is a mature capsid protein missing a signal sequence of the prM protein. The C2 protein was also detected in the other cell lines examined, and a further processed capsid protein was detected in N18 cells infected with JEV (Fig. 1B). It was shown that the JEV capsid protein is localized in the nuclei as well as in the cytoplasm of the infected cells (32). The C1 and C2 proteins were also detected in both the cytoplasmic and nuclear fractions (Fig. 1C). These results indicate that two forms of the capsid proteins, C1 and C2, are generated in cells infected with JEV, and the larger capsid (C1) is selectively incorporated into the viral particles.

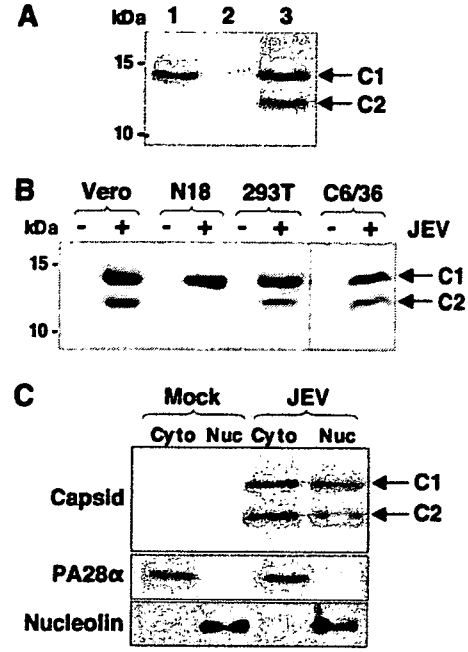

FIG. 1. Detection of C2 protein in cells infected with JEV. (A) Detection of the capsid proteins from the purified viral particles and cells infected with JEV. Lane 1, purified JEV particles produced in Vero cells; lanes 2 and 3, mock- and JEV-infected Vero cells, respectively. Arrows indicate a mature capsid protein (C1) and a further-processed capsid protein (C2). (B) Detection of the capsid protein from various cell lines infected with JEV. (C) Detection of the C1 and C2 proteins in the cytoplasmic (Cyto) and nuclear (Nuc) fractions of Vero cells infected with JEV. PA28-α and nucleolin are control proteins of the cytoplasmic and nuclear fractions, respectively.

The C2 protein lacks the amino terminus. To determine which terminus is missing in the C2 protein, expression plasmids encoding a series of capsid proteins with or without amino-terminal FLAG and carboxyl-terminal HA tags (F-JEC-H, F-JEC, JEC-H, and JEC) were generated (Fig. 2A). Both the C1 and C2 isoforms were detected in Vero cells transfected with each of the expression plasmids by immunoblotting with anti-JEV capsid PAb (Fig. 2B). The size of the C2 proteins in cells transfected with JEC was similar to that of F-JEC, which has the amino-terminal FLAG tag, whereas larger products were detected in the cells transfected with F-JEC-H and JEC-H, which have the carboxyl-terminal HA tag. Consistent with this observation, anti-HA antibody recognized both isoforms in cells expressing F-JEC-H and JEC-H, whereas anti-FLAG antibody detected only C1 in cells expressing F-JEC-H and F-JEC. These results indicate that the C2 protein lacks the amino-terminal region of the JEV capsid protein.

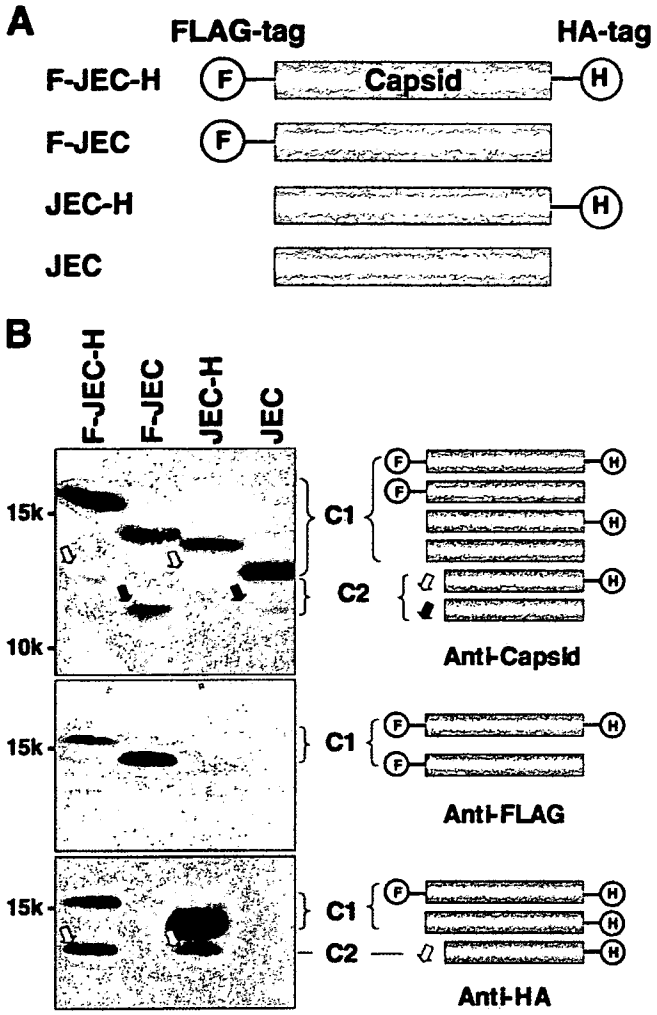

FIG. 2. The C2 protein lacks the amino terminus. (A) Series of the capsid protein constructs with or without FLAG and HA tags in the amino and carboxyl termini, respectively. (B) Expression of a series of the capsid proteins in Vero cells. The cell lysates expressing F-JEC-H, F-JEC, JEC-H, and JEC were examined by immunoblotting using anti-capsid, anti-FLAG, and anti-HA antibodies. The molecules detected by the immunoblotting are indicated on the right. White and black arrows indicate the C2 proteins with and without HA tags in the carboxyl terminus, respectively.

The JEV capsid protein is processed by cathepsin L. The C2 protein missing the amino-terminal region of the JEV capsid protein may be generated through cleavage by a host cell protease(s) or translation from the second start codon by leaky scanning, as reported in the case of DEN2 (9). To assess these possibilities, cells expressing F-JEC-H were treated with various protease inhibitors. C2 production was completely abrogated by treatment with broad-spectrum cysteine protease inhibitor E64d at the concentration of 50 μM, along with an increase in C1 expression (Fig. 3A), indicating that the JEV C2 protein was generated via cleavage of the C1 protein by a cysteine protease(s) but not leaky scanning. To identify the cysteine protease responsible for the processing of the JEV capsid protein, specific inhibitors for individual cysteine proteases were examined in cells expressing F-JEC-H. The inhibitors for cathepsins B and L, CA074Me (10 μM) (6) and Z-FY-DMK (10 μM) (40), impaired the processing, while an inhibitor of caspases, Z-VAD-FMK (20 μM), and an inhibitor of calpains, PD150606 (20 μM), exhibited no effect (Fig. 3A). Cathepsins B and L are known to be present in the late endosome and lysosome. The treatments with inhibitors of these acidic compartments, ammonium chloride (10 mM), chloroquine (50 μM), and bafilomycin A1 (100 nM), also blocked the processing of the capsid protein (Fig. 3B). To determine whether cathepsin B or L is a dominant protease for cleavage of the JEV capsid protein, the dose dependency of the effects of cathepsin inhibitors CA074Me and Z-FY-DMK on the cleavage of F-JEC-H was examined. The processing of the JEV capsid protein was inhibited in a manner that correlated closely with the inactivation of cathepsin L rather than that of cathepsin B (Fig. 3C). Furthermore, overexpression of cathepsin L, but not cathepsin B and inactive cathepsin L (C138A), resulted in an increase of C2 production in 293T cells (Fig. 3D). In addition, production of C2 from F-JEC-H was significantly decreased in two independent clones of Vero cells stably expressing siRNA for cathepsin L (Fig. 3E). These results indicate that cathepsin L is responsible for the processing of the JEV capsid protein to generate the C2 protein.

Identification of the site of the cleavage of the JEV capsid protein by cathepsin L. To determine the site of the cleavage of the JEV capsid protein by cathepsin L, a recombinant capsid protein possessing amino-terminal thioredoxin, His, and S tags and carboxyl-terminal myc and His tags was prepared (Fig. 4A). The in vitro incubation of the purified capsid protein with cathepsin L at room temperature for 60 min generated two major cleaved products, detectable by anti-myc antibody (Fig. 4B). The amino-terminal amino acid sequencing revealed that the mass of cleaved product 1 contained two peptides beginning with the residues Ser-Asp-Lys-Ile-Ile (a minor peptide) and Arg-Gln-His-Met-Asp (a major peptide), corresponding to a region of the thioredoxin and S tags, respectively (Fig. 4A and B). On the other hand, cleaved product 2 contained a single peptide beginning with Arg-Gly-Leu-Pro-Arg, corresponding to amino acid residues 19 to 23 of the JEV capsid protein. This result indicates that the JEV capsid protein is cleaved between Lys^{18} and Arg^{19} by cathepsin L in vitro (Fig. 4C). To further confirm the cleavage of the capsid protein in mammalian cells, a series of F-JEC-H proteins with alanine substitutions in each residue around the cleavage site (Ile^{14} to Arg^{23}) was expressed in Vero cells (Fig. 4D). As indicated in the reports that a hydrophobic amino acid residue at position P2 is responsible for the substrate specificity of cathepsin L (37, 38), the replacement of Leu^{17} (P2) with alanine was crucial for capsid protein processing. In addition, although the single replacements at the cleavage site of Lys^{18} (P1) and Arg^{19} (P1') with alanine had no effect on cleavage, the double substitution of acidic amino acids (Lys^{18} to Glu and Arg^{19} to Asp) resulted in impairment of C2 production (Fig. 4D). These results indicate that the JEV capsid protein is cleaved between Lys^{18} and Arg^{19} by cathepsin L in vitro and in vivo.

Production of the C2 proteins of DENs. The P4 to P1' region of the cathepsin L cleavage site is conserved among many mosquito-borne flaviviruses, including MVE, WNV, and DENs (Fig. 4C), and the 5'-complementary cyclization sequences are over-

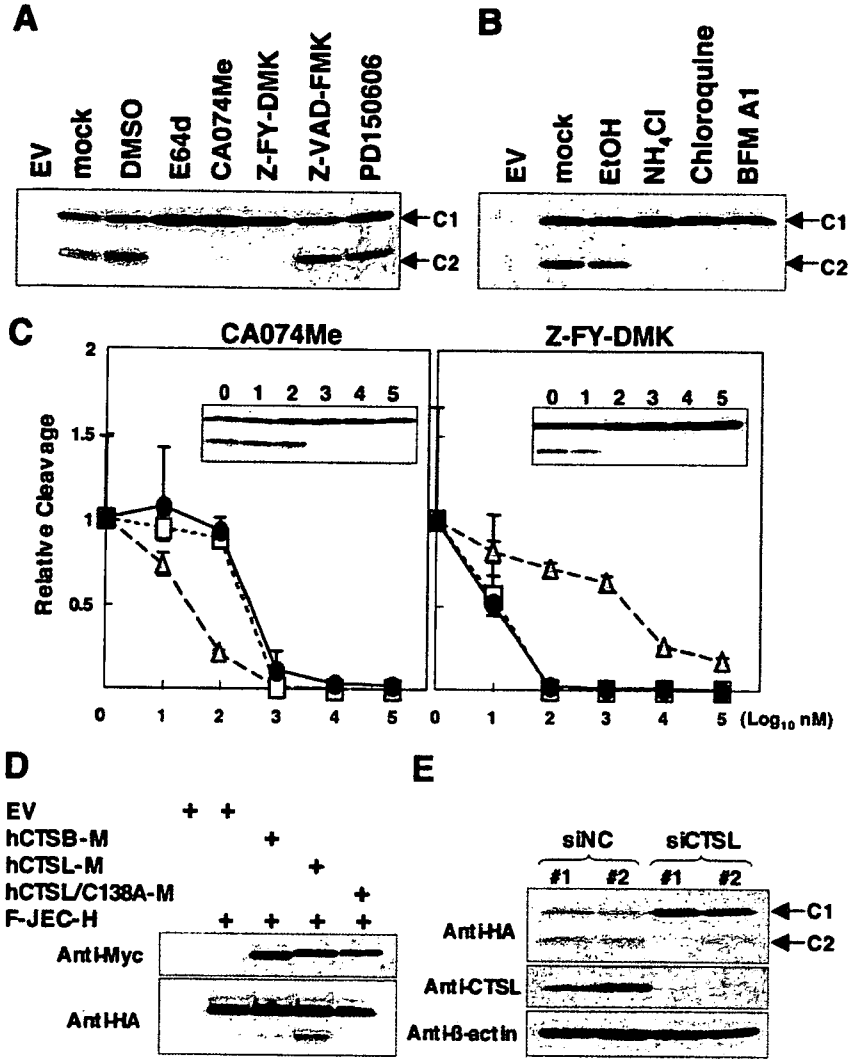

FIG. 3. JEV capsid protein is processed by cathepsin L. (A) Effects of cysteine protease inhibitors on the processing of the JEV capsid protein. Vero cells expressing F-JEC-H were treated with 50 μM E64d, 10 μM CA074Me, 10 μM Z-FY-DMK, 20 μM Z-VAD-FMK, or 20 μM PD150606 for 8 h at 37°C and examined by immunoblotting using an anti-HA antibody. EV, empty vector. (B) Effects of anti-acidic compartment reagents on the processing of the JEV capsid protein. Vero cells expressing F-JEC-H were treated with 10 mM ammonium chloride, 50 μM chloroquine, or 100 nM bafilomycin A1 (BFM A1) for 8 h at 37°C and examined by immunoblotting using an anti-HA antibody. EtOH, ethanol. (C) Dose-dependent effects of two cathepsin inhibitors, CA074Me and Z-FY-DMK, on F-JEC-H processing. Vero cells expressing F-JEC-H were treated with CA074Me or Z-FY-DMK at the indicated concentrations for 8 h at 37°C and examined by immunoblotting using an anti-HA antibody. The relative cleavage values for the capsid protein (solid circles) were calculated as the intensity of C2 compared to that of C1 in three independent experiments. A representative image of the immunoblotting is indicated in each graph panel. The relative levels of cleavage of the substrates specific to cathepsin B (gray triangles) and cathepsin L (open squares) were determined as described in Materials and Methods. The value for the control sample without treatment of each inhibitor was taken as 1. (D) Effects of the overexpression of cathepsins on the processing of the JEV capsid protein. 293T cells were cotransfected with plasmids encoding myc-tagged human cathepsin B (hCTSB-M), cathepsin L (hCTSL-M), or inactive cathepsin L (hCTSL/C138A-M) with F-JEC-H. Immunoblot analysis was carried out using the antibodies shown at the left. (E) Processing of F-JEC-H in Vero cells stably expressing hairpin siRNA corresponding to the negative control (siNC) or cathepsin L (siCTSL). Immunoblot analysis was carried out using the antibodies shown at the left.

lapped through the P4 to P2 sites (1, 19) (Fig. 5A). The C2 proteins were also detected in cells expressing the capsid proteins of DEN2 and DEN4 (Fig. 4E). To determine whether the C2 proteins of DEN are generated in the same manner as the C2 proteins of JEV, we examined the effect of the cysteine protease inhibitor E64d on the productions of the DEN C2 proteins. When cells were treated with E64d at a concentration of 50 μM, the C2 protein was diminished in cells expressing the capsid protein of JEV, but not in those expressing DEN2 and DEN4. However, it should be noted that treatment with the inhibitor induced a slight delay in migration of the C2 proteins of DENs. These results suggest that cysteine proteases do not play a major role in the production of the C2 proteins of DENs but play some roles in their processing.

Construction of a mutant JEV carrying the capsid protein resistant to cleavage by cathepsin L. To assess the biological significance of the cleavage of the JEV capsid protein by cathepsin L, a mutant JEV with Leu^{17} replaced by Ala (L17A)

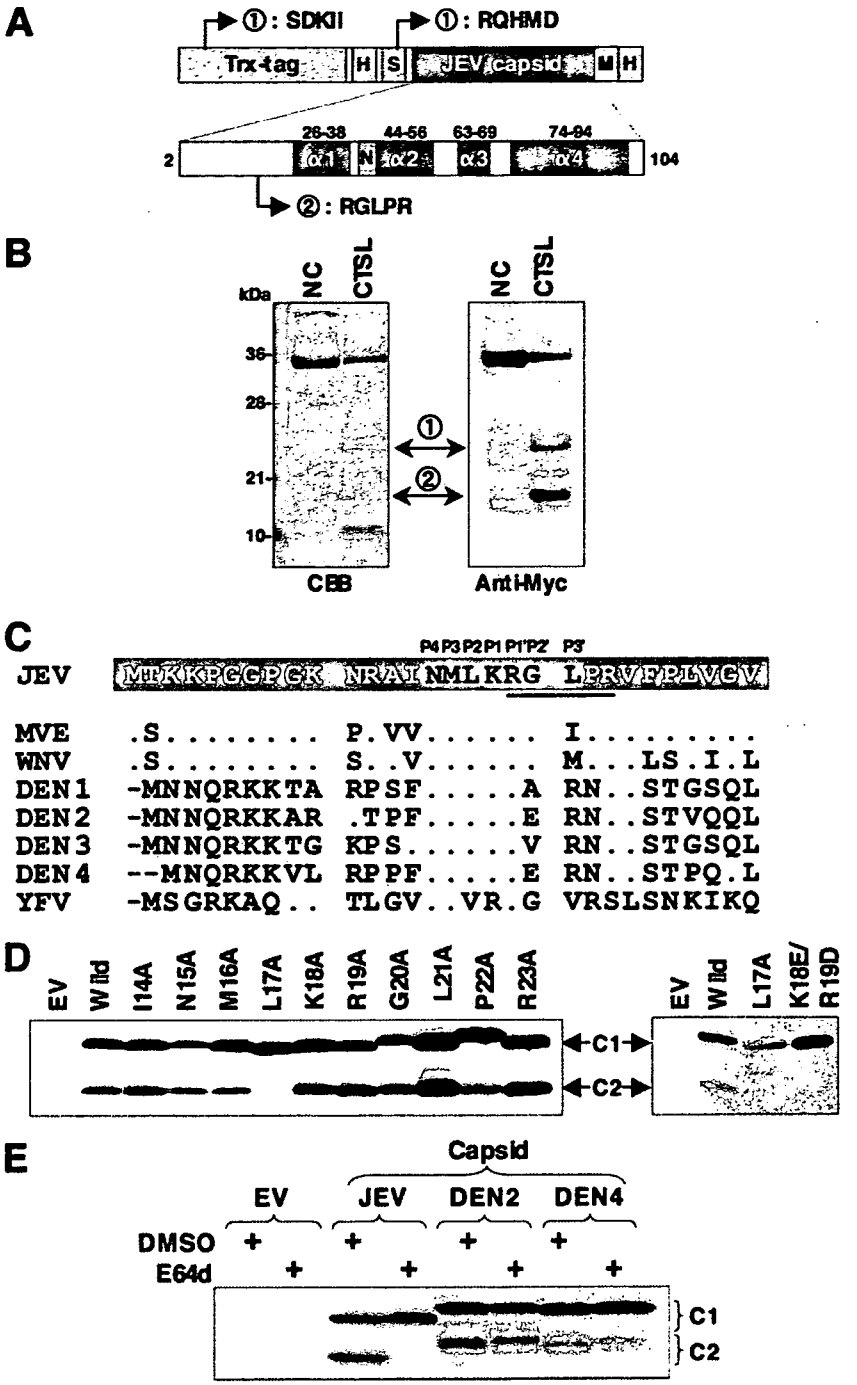

FIG. 4. Identification of the site of cleavage of JEV capsid protein by cathepsin L. (A) Schematic diagram of the recombinant JEV capsid protein. The His, S, and myc tags are indicated as H, S, and M, respectively. Four α-helices (α1 to 4) of the JEV capsid protein were predicted by Ma et al. (27). The nuclear localization signal (N) was mapped to residues Gly^{42} and Pro^{43} (32). Products 1 and 2 of in vitro cleavage by cathepsin L began at the indicated positions. Trx, thioredoxin. (B) The purified capsid protein (33 μg [1 nmol]/100 μl) was treated with 0.01 units of recombinant human cathepsin L (CTSL) at room temperature for 60 min and analyzed by Coomassie brilliant blue (CBB) staining and immunoblotting using an anti-myc antibody after SDS-PAGE. The amino-terminal amino acid sequences of cleavage products 1 and 2 were determined by the Edman degradation method. (C) Alignment of the amino-terminal amino acid sequences of the mosquito-borne flaviviral capsid proteins. Positions P4 to P3′ of the site of cleavage of the JEV capsid protein by cathepsin L are shown at the top of the sequences. The amino-terminal amino acid sequences of cleavage product 2 generated by cathepsin L in vitro are underlined. Identical and deleted residues compared with the JEV capsid protein are indicated as dots and bars, respectively. (D) Identification of crucial residues for capsid protein processing by cathepsin L in vivo. A series of the mutant constructs derived from F-JEC-H were expressed in Vero cells and analyzed by immunoblotting using an anti-HA antibody. (E) Effect of a cysteine protease inhibitor E64d on the processing of the DEN capsid proteins. Vero cells expressing the FLAG- and HA-tagged capsid proteins of JEV, DEN2, and DEN4 were treated with DMSO or 50 μM E64d for 8 h at 37°C and examined by immunoblotting using an anti-HA antibody.